NATIONAL ADVISORY COMMITTEE FOR AERONAUTICS

TECHNICAL NOTE

No. 1055

COMPARISON OF TWO-DIMENSIONAL AIR FLOWS ABOUT AN NACA 0012 AIRFOIL OF 1-INCH CHORD AT ZERO LIFT IN OPEN AND CLOSED 3-INCH JETS AND CORRECTIONS FOR JET-BOUNDARY INTERFERENCE

By Ray H. Wright and Coleman duP. Donaldson

Langley Memorial Aeronautical Laboratory
Langley Field, Va.

Washington
May 1946

NATIONAL ADVISORY COMMITTEE FOR AERONAUTICS

TECHNICAL NOTE NO. 1055

COMPARISON OF TWO-DIMENSIONAL AIR FLOWS ABOUT AN NACA 0012 AIRFOIL OF 1-INCH CHORD AT ZERO LIFT IN OPEN AND CLOSED 3-INCH JETS AND CORRECTIONS FOR JET-BOUNDARY INTERFERENCE

By Ray H. Wright and Coleman duP. Donaldson

SUMMARY

Pressure distributions and schlieren photographs for the high-speed flow about a symmetrical airfoil at zero lift in open and closed jets are analyzed to show the nature of the jet-boundary interference. Application of the theoretical tunnel-wall corrections brought the results for the open-throat and closed-throat tunnels into approximate agreement. The stream Mach number in the closed jet was limited by tunnel choking. In the open jet, although the theoretical interference was less than in the closed jet, unsteadiness connected with the jet-boundary conditions limited the usefulness of the results at high Mach numbers.

INTRODUCTION

In order to correlate wind-tunnel data with the free-flight performance of aircraft, corrections for the influence of the free or solid boundaries of the tunnel air stream must be applied or must be shown to be negligible. Theoretical corrections applicable with incompressible flow have long been known and have been checked by experiment. Theory for the effect of compressibility on the corrections has recently been developed, but this theory has not been fully verified by experiment nor have the limits of applicability of the theory been established. The tests of this investigation of an NACA 0012 airfoil in open-throat and closed-throat tunnels were expected to indicate the applicability of the theoretical compressibility

effect on the solid-constriction correction and to establish the order of magnitude of the solid-constriction correction at the highest Mach number attainable in the closed tunnel. Inasmuch as the theoretical solid-constriction corrections are of opposite sign for open-throat and closed-throat tunnels, the coincidence of the theoretically corrected results for an airfoil tested in open and closed jets of the same size would constitute evidence of the validity of the theoretical corrections. In the theory employed in the analysis of the data, the dimensions of the model are assumed to be small in comparison with those of the tunnel. The experimental arrangement satisfied this assumption. The experimental work was done in the Langley 1-inch turbine-element testing apparatus, for which in these tests the throat was 1 by 3 inches.

SYMBOLS

t	model thickness
c	model chord
λ	parameter depending on airfoil base profile shape
h	tunnel height, distance between upper and lower walls of jet
x, y	Cartesian coordinates, orientation defined where used
r, θ	polar coordinates, orientation defined where used
p	static pressure
H	total pressure
V	velocity
ΔV	velocity increment
a	speed of sound
M	Mach number, value in the undisturbed stream unless otherwise indicated (V/a)

ΔM Mach number increment

R Reynolds number

γ ratio of specific heat at constant pressure to specific heat at constant volume for air

α angle of attack

c_d section drag coefficient

Subscripts:

i incompressible

c compressible

o undisturbed stream

a at orifice a

b at orifice b

1 increment at orifices a and b due to first pair of doublet images (images A and A' of fig. 7)

2 increment at orifices a and b due to second pair of doublet images (images B and B' of fig. 7)

3 increment at orifices a and b due to all doublet images except first two pairs

4 total increment at orifices a or b due to all doublet images

5 total increment at position of model due to all doublet images

av average value between orifices a and b

ch choking

l local

corr values with solid-constriction corrections applied

cr critical value corresponding to first attainment of speed of sound in flow field

eff effective value (all corrections applied including direct model interference at calibration orifices)

APPARATUS AND METHODS

Because schlieren photographs of the entire flow field about the model airfoil in the tunnel were desired, the apparatus used to simulate both the open-throat and the closed-throat tunnel was of necessity quite small. The test apparatus is shown in figure 1.

A supply of compressed air, valved into the settling chamber, was passed through a number of fine screens and was contracted into the test section. The upper and lower walls of the test section were interchangeable wooden blocks shaped to simulate either an open-throat or a closed-throat tunnel. The vertical walls were also interchangeable. The test airfoil equipped with pressure-distribution orifices could be mounted between steel plates that were also equipped with pressure orifices (see fig. 2) for measuring the flow velocities and for setting the angle of attack. This setup was provided with a simple yoke mechanism (fig. 1) so that the angle of attack could be adjusted while the tunnel was in operation. The steel plates could be replaced by plate-glass frames so that the entire field of flow could be photographed by use of a schlieren technique. For the schlieren photographs, the airfoil was held in place mainly by friction and the angle of attack was adjusted between runs by trial and error.

The model used was an NACA 0012 airfoil of 1-inch span and 1-inch chord. One surface was equipped with nine pressure orifices at points 7.5, 17.5, 27.5, 37.5, 47.5, 57.5, 67.5, 77.5, and 87.5 percent chord from the leading edge. The tunnel height for both the open-throat and closed-throat tunnels in all tests was 3 inches. The ratio of the model thickness to the tunnel height was thus $\frac{t}{h} = 0.04$ and appreciable tunnel corrections would be expected even at low speeds. With this arrangement the Reynolds number at the airfoil critical speed was approximately 350,000.

Mach numbers M at various points in the tunnel were obtained from the total pressure H and the static pressure p by use of the relation

$$M = \sqrt{\frac{2}{\gamma - 1}\left[\left(\frac{H}{p}\right)^{\frac{\gamma-1}{\gamma}} - 1\right]} \qquad (1)$$

where γ is the ratio of specific heats. By means of a calibration, the total pressure was known as a function of the pressure in the settling chamber; the static pressures were measured in the usual way by means of a manometer.

The tunnel Mach number was taken as that corresponding to the pressure at orifice a, which was in the tunnel side wall at a point 1.375 inches upstream from the leading edge of the model (fig. 2). Pressure distributions at the surface of the model were taken at tunnel Mach numbers ranging from 0.35 to 1.0 in the open jet and from 0.35 to 0.797, which was the choking Mach number, in the closed jet. The pressure at orifice b, which was in the tunnel side wall at a point 1.375 inches downstream from the trailing edge (fig. 2), was also measured.

The angle of attack was adjusted to 0° by accurately balancing the pressures at two orifices symmetrically located above and below the airfoil (fig. 2). The adjustment was made on a sensitive alcohol manometer and at a tunnel Mach number of 0.60.

Schlieren photographs of the flow in both open and closed jets were made for the same Mach number ranges as those of the pressure-distribution tests but were not taken simultaneously with these. The schlieren method (method of striae) is described in reference 1. In the present tests, lenses were replaced with mirrors.

TEST RESULTS

The pressure distributions are presented as the ratios of the local static pressure to the total pressure p_l/H. The pressure ratios plotted against the distance from the leading edge expressed in terms of

the chord for various tunnel Mach numbers M_a in the closed tunnel are given in figure 3. A similar plot for the open jet is presented in figure 4. The orifices at 17.5, 47.5, and 67.5 percent chord were found to be plugged or leaking and the pressures at these orifices are therefore not presented. Additional pressure data were taken in the open jet but were found to be incomplete and could not be analyzed.

The schlieren photographs of the flow about the airfoil in the closed and open jets are shown as figures 5 and 6. The Mach numbers for these figures are the tunnel Mach numbers M and the angle of attack is 0°. The schlieren setup was so arranged that light regions indicate increasing density downstream (compression) and dark regions, decreasing density downstream (expansion). Because a shock wave is a compression, it appears as a light line often followed by a parallel dark strip. The photographs of figures 5(f), 5(i), 5(j), 5(o), and 5(p) were taken with the schlieren system adjusted for greater sensitivity than it was for the other photographs of the series. In the photographs of the model in the closed jet (fig. 5), the upper and lower boundaries of the photographs represent the tunnel walls. In the photographs of the model in the open jet (fig. 6), the upper and lower boundaries are shown by vortex sheets. In all schlieren photographs the flow direction is from left to right.

ANALYSIS AND DISCUSSION

Application of Jet-Boundary-Interference Theory

The theory used in the analysis of the data is contained in the references and is not repeated herein; the application of the theory is, however, described. The following corrections must be applied: (a) a correction for the tunnel-wall interference at the position of the model, (b) a correction for the interference of the model at the calibration orifices used for determining the tunnel velocity and Mach number, and (c) a correction for the wall interference at these orifices. In addition, for the present tests, the existence of a pressure gradient in the tunnel is taken into account along with the corrections due to interference. The theoretical

tunnel-wall interference at the position of the model is treated first and the order of magnitude of the corrections involved is investigated. The influence of the model alone at the calibration orifices is discussed next. The pressure gradient and part of the wall interference are then shown to be approximately taken into account by averaging the pressures between calibration orifices equidistant from the leading and trailing edges of the model. Finally, the remaining part of the interference at the calibration orifices and at the model is calculated and the corrections applied.

Theoretical tunnel-wall interference.- Two types of wall interference, solid constriction and wake constriction, affect the two-dimensional subsonic flow about a symmetrical airfoil at zero lift in a tunnel with solid boundaries. The presence of the rigid boundaries prevents the lateral expansion of the flow and thus increases the effective stream velocities (and Mach numbers) in the vicinity of the model. This type of wall interference is referred to herein as "solid constriction." The wake due to the airfoil drag occupies a region of low velocity behind the airfoil. Again the rigid boundaries prevent lateral expansion such as would occur in an infinite stream and the continuity condition of constant mass flow through all cross sections of the tunnel requires that the velocity outside the wake be greater than if the wall constriction did not occur. This effect is termed "wake constriction." Both types of interference result in an effective increase in velocity and Mach number at the model. For a symmetrical airfoil at zero lift, the assumption is made in the theory that a correction to the indicated tunnel velocity is the only tunnel-wall correction required. The density, dynamic pressure, Mach number, and Reynolds number must, of course, be corrected accordingly.

In a tunnel with free boundaries, the lateral expansion of the flow about the airfoil is greater than in an infinite stream and the velocity in the vicinity of the airfoil is therefore reduced. The magnitude of the solid-constriction correction in an open jet is only one-half that in the closed jet and the wake constriction is negligible.

The tunnel-wall-correction theory applicable with incompressible flow is developed in reference 2,

pages 50 to 57. The solid-constriction correction, that is, the velocity increment ΔV to be added to the indicated tunnel velocity, is shown to be, for the closed-throat tunnel,

$$\frac{\Delta V}{V_o} = \frac{\pi^2}{12} \lambda \left(\frac{t}{h}\right)^2 \qquad (2)$$

and, for the open-throat tunnel,

$$\frac{\Delta V}{V_o} = -\frac{\pi^2}{24} \lambda \left(\frac{t}{h}\right)^2 \qquad (3)$$

where

V_o tunnel velocity

t thickness of airfoil

h tunnel height

λ parameter depending on airfoil shape

With compressible flow, formulas (2) and (3) suffer important changes due to compressibility effects. The most complete available theory of the compressibility effects on two-dimensional tunnel-wall interference is contained in reference 3, in which the velocity-interference corrections for solid constriction in the closed jet are shown to vary as $\frac{1}{(1 - M^2)^{3/2}}$. The theory of reference 3 is applicable also to the solid constriction in the open-throat tunnel and the compressibility effect in the open jet is the same as that in the closed jet. In compressible flow, formulas (2) and (3) therefore become, for the closed-throat tunnel,

$$\frac{\Delta V}{V_o} = \frac{\lambda}{(1 - M^2)^{3/2}} \frac{\pi^2}{12} \left(\frac{t}{h}\right)^2 \qquad (4)$$

and, for the open-throat tunnel,

$$\frac{\Delta V}{V_o} = \frac{-\lambda}{(1 - M^2)^{3/2}} \frac{\pi^2}{24} \left(\frac{t}{h}\right)^2 \qquad (5)$$

where M is the stream Mach number corresponding to V_o.

The wake-constriction correction for the closed-throat tunnel with the compressibility effect included, as taken from equation (23) of reference 3, is

$$\frac{\Delta V}{V_o} = \frac{1 + 0.4M^2}{1 - M^2} \frac{c_d c}{4h} \qquad (6)$$

where c_d is the section drag coefficient based on the airfoil chord c. Within the accuracy of the other approximations employed herein, the apparent value of c_d rather than the corrected value may be used. The solid-constriction correction decreases very rapidly as the size of the model is decreased, for this correction is proportional to the square of the ratio of the model dimensions to tunnel height; the wake-constriction correction decreases much less rapidly, for it varies as the first power of the ratio of model dimensions to tunnel height. It will be observed that the theoretical compressibility correction for wake constriction is different from that for solid constriction.

An estimate can now be made of the relative magnitude of the two corrections in the closed jet with a low value of the Mach number. With a Mach number of 0.5, the velocity is approximately 380 miles per hour, which corresponds to a Reynolds number for the 1-inch-chord airfoil under standard conditions of about $R = 295{,}000$, or $\log R = 5.47$. From figure 148 of reference 4 the drag coefficient c_d at this Reynolds number is of the order of 0.01. With $c = 1$ inch and $h = 3$ inches, equation (6), when the effect of compressibility is not taken into account, is

$$\frac{\Delta V}{V_o} = \frac{c_d c}{4h}$$

$$= \frac{0.01 \times 1}{4 \times 3}$$

$$= 0.00083 \qquad (7)$$

For the NACA 0012 airfoil, $\lambda = 4.12$ (reference 3) and the thickness of the 1-inch-chord airfoil is 0.12 inch so that the solid-constriction correction given by equation (2) is

$$\frac{\Delta V}{V_o} = \frac{\pi^2}{12} \lambda \left(\frac{t}{h}\right)^2$$

$$= 0.00542 \qquad (8)$$

The estimated solid-constriction correction is nearly seven times the estimated wake-constriction correction. At Mach numbers larger than the critical, however, the drag may increase greatly and the size of the solid-constriction correction may be exceeded by that of the wake-constriction correction.

The corrections in equations (4) to (6) are to be applied to the velocity in a parallel channel without boundary layer and at an infinite distance upstream from the model, where the influence of the model is negligible. Practically, the effect of the boundary layer is kept small by limiting the length of the test section of the tunnel, for the boundary layer is prevented in this way from becoming very thick, and corrections are applied for any velocity gradient produced by boundary-layer development or wall divergence or both. In any practical case, however, the influence of the model at the orifices used to determine the tunnel velocity may not be negligible, and account must be taken of this interference.

Influence of model alone on velocities at calibration orifices.- In the present tests the tunnel velocities were determined from measurements taken at orifices a and b as previously described. (See fig. 2.) Consider the consequences of basing velocities and Mach numbers on pressures taken at these orifices. Suppose first that the airfoil is placed in an infinite, uniform stream of velocity V_o. The airfoil can be represented by a distribution of sources and sinks of total strength zero. With such a distribution representing the NACA 0012 airfoil, the velocities for incompressible flow at orifices a and b were found to be

$$\left(\frac{\Delta V}{V_o}\right)_{i_a} = -0.0048 \qquad (9)$$

and

$$\left(\frac{\Delta V}{V_o}\right)_{i_b} = -0.0040 \qquad (10)$$

From the first of equations (A10) of reference 3, these increments are expected to increase with Mach number by the factor $\frac{1}{\sqrt{1 - M^2}}$.

The velocities at orifices a and b are affected by the wake also. It is reasonable to suppose that the effect of the wake may be represented by a distribution of sources, sinks, and vortices. The vorticity coming off the upper surface is equal in magnitude but opposite in sign to that coming off the lower surface and the positive and negative vorticities rapidly diffuse so that, if the wake is not excessively large and violently fluctuating, the effect of the vorticity a short distance from the airfoil is negligible. The sink distribution as shown in part II of reference 5 is due to the wake dissipation behind the airfoil. At a considerable distance from the airfoil, the combination of sources and compensating sinks has approximately the same effect as a doublet. In the representation of the wake, however, the sources exceed the sinks by $\frac{V_o c_d c}{2}$ (reference 5, part II). Because the sum of the compensated sinks

cannot be as great as this value and because the induced velocities due to a source and to a doublet vary inversely as the first and second powers of the distance from the position of the source and doublet, respectively, the velocities induced by the wake at orifices a and b are due mainly to the source of strength $\frac{V_o c_d c}{2}$.

If, instead of a source distribution, a single source of strength $\frac{V_o c_d c}{2}$ is assumed to be concentrated at the midpoint of the airfoil chord, the induced velocities at orifices a and b with the previously estimated drag coefficient of 0.01 are (including the compressibility effect given by equations (A10) and (20) of reference 3)

$$\left(\frac{\Delta V}{V_o}\right)_a = \frac{1 + 0.4M^2}{\sqrt{1 - M^2}} \frac{c_d c}{4\pi x}$$

$$= \frac{1 + 0.4M^2}{\sqrt{1 - M^2}} \frac{0.01(1)}{4\pi(-1.875)}$$

$$= -0.000442 \frac{1 + 0.4M^2}{\sqrt{1 - M^2}} \qquad (11)$$

and

$$\left(\frac{\Delta V}{V_o}\right)_b = \frac{1 + 0.4M^2}{\sqrt{1 - M^2}} \frac{0.01(1)}{4\pi(1.875)}$$

$$= 0.000442 \frac{1 + 0.4M^2}{\sqrt{1 - M^2}} \qquad (12)$$

where x is the distance from the source measured positive along the chord in the direction of the free-stream velocity V_o. Because of the increase in drag coefficient, these velocity increments may be greatly increased at Mach numbers larger than the critical but

will still be small in comparison with the stream velocity. With small induced velocities, the pressure differences are proportional to the velocity increments and, because the induced velocities at orifices a and b due to the source at the origin are opposite in sign, the velocities and Mach numbers computed from the average of pressures at orifices a and b are automatically compensated for the effect of the wake at the measuring orifices. Because the effect of the actual wake may not be accurately represented by a source at the origin, the wake effect will not be exactly compensated but, at least with Mach numbers less than the critical, the error involved is believed to be small. Correction for the error given by equations (9) and (10), which involves addition of a velocity increment

$$\frac{\Delta V}{V_o} = \frac{0.0048 + 0.0040}{2\sqrt{1 - M^2}} \qquad (13)$$

to the stream velocity determined from the average of pressures at orifices a and b, should therefore yield a good approximation to the true velocity of the infinite stream.

Corrections for wake and wake-constriction interference and for pressure gradient.- Suppose now the airfoil is placed in a closed-throat wind tunnel. As shown in reference 6, the wall interference due to wake constriction can be represented by means of source images in the tunnel walls. The velocities at orifices a and b will be affected by these images as well as by the source representing the original wake. From equations (21), (23), and (25) of page 34 of reference 6, the velocity at orifice b due to the source $\frac{V_o c_d c}{2}$ and its images is

$$\frac{\Delta V}{V_o} = \frac{c_d c}{4\pi} \frac{\pi}{2h} \left(\coth \frac{\pi x}{2h} + \tanh \frac{\pi x}{2h} \right) \qquad (14)$$

or with $c_d = 0.01$, $c = 1$ inch, $h = 3$ inches, and $x = 1.875$ inches

$$\frac{\Delta V}{V_o} = \frac{0.01}{24}(1.326 + 0.754)$$

$$= 0.00087 \qquad (15)$$

which is about twice the value obtained without the wall interference. At orifice a the induced velocity due to the wake and its images is the negative of the value given in equation (15). Because the angle between the stream direction and the radius vector from any image is the same for orifice a as for orifice b, the compressibility effect given by equations (All) and (20) of reference 3 is also the same and the velocity increments remain equal in magnitude but opposite in direction so that, as in the case of the infinite stream, the effect of the wake is removed by averaging the Mach numbers at orifices a and b.

In the open jet, the source images must be alternately negative and positive and the effect of the wake is given by taking the hyperbolic tangent term negative in equation (14) so that at orifice b

$$\frac{\Delta V}{V_o} = \frac{0.01}{24}(1.326 - 0.754)$$

$$= 0.00024 \qquad (16)$$

The induced velocity at orifice a is the negative of this value (because x is negative ahead of the model). The compressibility effect is again the same at orifice a as at orifice b and again the effect of the wake is removed by averaging values at orifices a and b.

An estimate of the effect of basing the tunnel velocity on the average value of the pressures at orifices a and b, if the source representing the wake were located at the trailing edge instead of at the center of the chord as assumed, indicated an error of about one-fifth of the total wake-constriction correction. Inasmuch as the effective origin of the wake should lie between the center and the trailing edge, the error due to the excentral origin of the wake should therefore be less than the estimated one-fifth.

A more serious source of error is the pressure gradient that exists in the tunnel without the model. This pressure gradient is usually taken into account by means of an empty-tunnel calibration but, in the present case, an empty-tunnel calibration was not available and therefore direct corrections for the pressure gradients could not be made. The pressure gradients, moreover, are thought to have varied from test to test because the open-throat and closed-throat tunnels were taken down and reassembled several times without any check on the pressure gradients. If the gradient is constant, the method of averaging pressures between orifices a and b will eliminate the effect of the gradient on the determination of the velocity and Mach number at the model. If the gradient is not constant, the estimated velocity will be too high or too low, depending on whether the velocity gradient is increasing or decreasing.

In this analysis, the assumption is made that the average of the pressures at orifices a and b corresponds to a velocity at the model which is automatically corrected for wake constriction and pressure gradient. The only correction to be applied to the velocity so obtained is that due to the effect of the airfoil profile and its images.

Correction for interference due to profile.- The correction to be applied to the average of the velocities at orifices a and b is the difference between the velocity increment at the position of the model due to the solid constriction and the velocity increments at calibration orifices a and b due to the solid constriction plus the direct influence of the profile. The velocity increment at orifices a and b due to the solid constriction will be calculated first. As shown in reference 2, if the airfoil is small in comparison with the tunnel size, the boundary conditions can be approximately satisfied by means of an infinite series of images of the equivalent airfoil doublet in the tunnel boundaries. From reference 2, the equivalent doublet due to the airfoil is

$$\mu = \frac{\pi}{2} \lambda t^2 V_o \qquad (17)$$

and therefore, as seen from reference 7, with incompressible flow the induced velocity ΔV in the stream direction at a point (x,y) (see fig. 7) relative to any doublet image is

$$\frac{\Delta V}{V_o} = \frac{\frac{\pi}{2}\lambda t^2}{2\pi} \frac{y^2 - x^2}{\left(x^2 + y^2\right)^2} \tag{18}$$

The induced velocity due to the solid constriction at orifice a is the same as that at orifice b. Consider therefore the induced velocity at orifice b due to the images in the boundaries.

From equations (21), (23), (26), and (30) on pages 34 and 35 of reference 6, the incompressible-flow induced velocity on the x-axis due to the images of a doublet oriented in the direction of the flow in a closed channel is

$$\frac{\Delta V}{V_o} = a_1 \frac{\pi^2}{4h^2}\left(\operatorname{sech}^2 \frac{\pi x}{2h} - \operatorname{csch}^2 \frac{\pi x}{2h} + \frac{4h^2}{\pi^2 x^2}\right) \tag{19}$$

where, in the notation of this paper,

$$a_1 = \frac{\lambda t^2}{4}$$

With $t = 0.12$ inch, $x = 1.875$ inches, and $h = 3$ inches,

$$\frac{\Delta V}{V_o} = \frac{2}{16}\lambda\left(\frac{t}{h}\right)^2 (0.4317 - 0.7598 + 1.037)$$

$$= 0.437\lambda\left(\frac{t}{h}\right)^2 \tag{20}$$

The only change in equation (19) required for the open jet is to make the sech^2 term negative and

$$\frac{\Delta V}{V_o} = \frac{\pi^2}{16}\left(\frac{t}{h}\right)^2\left(-0.4317 - 0.7598 + 1.037\right)$$

$$= -0.095\lambda\left(\frac{t}{h}\right)^2 \qquad (21)$$

Because the compressibility effect varies with the angle θ (see fig. 7) between the x-axis and the radius vector from the doublet to the point considered, the contributions of the images must be divided in such a manner as to facilitate the application of the compressibility factors. From the theory of reference 8, the compressibility effect on the axial velocity due to the doublet is found to be

$$\frac{\Delta V_c}{\Delta V_i} = \frac{1 - M^2\,\dfrac{\sin^2\theta}{2\sin^2\theta - 1}}{\sqrt{1 - M^2}\left(1 - M^2\sin^2\theta\right)^2} \qquad (22)$$

For images A and A', which are 3 inches from the tunnel center line (see fig. 7), the term $\sin^2\theta$ is

$$\sin^2\theta = \frac{(3)^2}{(3)^2 + (1.875)^2}$$

$$= 0.719$$

Similarly for the next two images, B and B',

$$\sin^2\theta = \frac{(6)^2}{(6)^2 + (1.875)^2}$$

$$= 0.911$$

For the images 9 inches and more from the center line, $\sin^2\theta$ approaches unity and, because the maximum Mach number at which comparisons between values for open and closed jets can be made in these tests is about 0.85, the compressibility effect given by equation (22) is evidently approximated by $\frac{1}{(1 - M^2)^{3/2}}$. The induced velocity at orifice b may therefore be computed as: (a) that due to the first two images, A and A', plus (b) that due to the next two images, B and B', plus (c) that due to all other images. With $x = kh$ and $y = nh$, the induced velocity at orifice b due to images A and A' ($n = 1$, $k = 0.625$) taken together is thus, from equations (18) and (22)

$$\frac{\Delta V_1}{V_o} = (\pm)\frac{\lambda}{2}\left(\frac{t}{h}\right)^2 \frac{n^2 - k^2}{(k^2 + n^2)^2} \frac{1 - M^2 \dfrac{\sin^2\theta}{2\sin^2\theta - 1}}{\sqrt{1 - M^2}\left(1 - M^2 \sin^2\theta\right)^2}$$

$$= (\pm)\frac{0.157\lambda(t/h)^2(1 - 1.64M^2)}{\sqrt{1 - M^2}(1 - 0.72M^2)^2} \qquad (23)$$

where the positive sign applies for the closed-throat tunnel and the negative for the open-throat tunnel. The velocity due to the images at B and B' ($n = 2$, $k = 0.625$) is similarly

$$\frac{\Delta V_2}{V_o} = \frac{0.094\lambda(t/h)^2(1 - 1.11M^2)}{\sqrt{1 - M^2}\,(1 - 0.91M^2)} \qquad (24)$$

where the positive sign applies for both open-throat and closed-throat tunnels.

The contribution due to the remaining images is obtained by subtracting that due to images A, A', B, and B' (equations (23) and (24)) for incompressible flow ($M = 0$) from equations (20) and (21) for closed

and open jets, respectively, and dividing by the compressibility factor $(1 - M^2)^{3/2}$. For the closed jet, therefore,

$$\frac{\Delta V_3}{V_o} = \frac{(0.437 - 0.157 - 0.094)\lambda(t/h)^2}{(1 - M^2)^{3/2}}$$

$$= \frac{0.186\lambda(t/h)^2}{(1 - M^2)^{3/2}} \tag{25}$$

and, for the open jet,

$$\frac{\Delta V_3}{V_o} = \frac{(-0.095 + 0.157 - 0.094)\lambda(t/h)^2}{(1 - M^2)^{3/2}}$$

$$= \frac{-0.032\lambda(t/h)^2}{(1 - M^2)^{3/2}} \tag{26}$$

The total induced velocity at orifice b (or at orifice a) due to the solid constriction is therefore

$$\frac{\Delta V_4}{V_o} = \frac{\Delta V_1}{V_o} + \frac{\Delta V_2}{V_o} + \frac{\Delta V_3}{V_o} \tag{27}$$

The solid constriction, at the position of the model, given by equations (4) and (5) is, for the closed-throat tunnel,

$$\frac{\Delta V_5}{V_o} = \frac{0.822}{(1 - M^2)^{3/2}} \lambda \left(\frac{t}{h}\right)^2 \tag{28}$$

and, for the open-throat tunnel,

$$\frac{\Delta V_5}{V_o} = \frac{-0.411}{(1 - M^2)^{3/2}} \lambda \left(\frac{t}{h}\right)^2 \qquad (29)$$

The residual solid-constriction correction to be applied to the velocity averaged between orifices a and b, V_{av}, is therefore

$$\frac{\Delta V}{V_{av}} = \frac{\Delta V_5}{V_o} - \frac{\Delta V_4}{V_o} \qquad (30)$$

Addition to equation (30) of the velocity increment due to the direct influence of the profile at the calibration orifices, equation (13), completes the correction and yields the true effective velocity at the position of the model.

For any small velocity correction ΔV, a corresponding Mach number correction ΔM can be obtained from the relation

$$\frac{\Delta M}{M} = \frac{\Delta V}{V} \left(1 + \frac{\gamma - 1}{2} M^2\right) \qquad (31)$$

where for air $\gamma = 1.40$. This equation is easily derived by substituting equation (30) of reference 3 into the first equation on page 19 of the same report, expanding the equation, and neglecting powers of $\Delta V/V$ higher than the first.

Limitations to application of theory.- Several limitations to the application of the theory used in this analysis should be recognized. First, because the theory is based on subsonic potential flow and in view of the fact that, as the Mach number increases beyond the critical value, the flow departs increasingly from potential flow and that supersonic-flow regions appear in the field, a progressive divergence from the theory

in the supercritical flow regime might be expected. Application of the theoretical correction at Mach numbers greater than the critical can therefore be justified only by experiment.

A second limitation to the application of the theory is imposed by the fact that in the development of the theory the corrections were assumed to be small; powers of the velocity increments higher than the first were therefore neglected and the Mach numbers involved in the compressibility factors were assumed to be equal to those obtained from the tunnel calibration. At high Mach numbers the compressibility effects are such that the corrections may become large, even for relatively small values of the ratio of model thickness to tunnel height t/h, and the compressibility factors themselves may become inaccurate because of the uncertainty concerning the correct value of Mach number to use. If the correction becomes large, moreover, it may no longer be possible to correct the results by the simple process of correcting the stream velocity.

A severe limitation to the use of the closed tunnel is that of choking, which is described in reference 3. The choking Mach number, which is the highest Mach number attainable in a parallel channel far upstream from the model, is reached when the speed everywhere along some line across the channel is equal to the speed of sound. The line at which $M = 1.0$ commonly extends from the airfoil surfaces somewhere near the maximum thickness to the walls. If the line of $M = 1.0$ is straight and perpendicular to the axis of the channel, the choking Mach number M_{ch} is theoretically a maximum and is related to the thickness-to-height ratio t/h by

$$\frac{t}{h} = 1 - \frac{M_{ch}}{\left(1 + \frac{M_{ch}^2 - 1}{6}\right)^3} \qquad (32)$$

which is adapted from equation (87) of reference 3. Practically, the thinning of the boundary layer produced by the velocity increase at the walls due to the airfoil may permit the attainment of a somewhat higher value of the choking Mach number than is given by equation (32).

The effect of the absolute thickness of the boundary layer is small in comparison with the effect of the changes in the thickness. As the choking Mach number is approached, the tunnel-wall corrections are expected to become increasingly inaccurate. After the choking Mach number has been reached, the pressure differences between points upstream and downstream from the model can be increased without any appreciable change in the upstream Mach numbers. Because a single indicated tunnel Mach number corresponds to an infinite number of downstream pressure distributions, after the choking Mach number is reached, the conditions in the tunnel cannot be related to the tunnel Mach number and the application of corrections is obviously impossible.

Analysis of Experimental Wall-Interference Data and Comparison with Theory

Mach number distributions.- The experimental data are analyzed in terms of the local Mach numbers M_l that are related to the local pressures p_l of figures 3 and 4 by equation (1). These values of Mach number are assumed to be correct as determined from the measured pressures and to require no correction. Only the stream Mach numbers M at which the local Mach numbers M_l are plotted must be corrected.

For the tests in the open and closed jets, the values of M_l at each measuring point on the profile were first plotted against the indicated stream Mach numbers at orifice a, M_a. At chosen values of M_a values of M_l were taken from these curves and are shown plotted against chordwise location in figure 8. Except for the values for the closed-jet tests at $\frac{x}{c} = 0.075$, which are evidently in error, the local Mach numbers in the closed jet exceed those in the open jet. This behavior accords with the theory in that for the same indicated Mach number M_a the predicted effective stream Mach number is greater for the closed than for the open jet.

The possibility of correcting the test results for the open and closed jets by correcting only the stream Mach numbers depends on the existence of identical local

Mach number distributions for the two cases at corresponding but different values of M_a. These two values of M_a for the open and closed jet then correspond to some single effective value of the stream Mach number. If the M_l-curves for the open and closed jets coincide at given values of the theoretically corrected stream Mach number, the theory may be assumed to be correct and the effective Mach number to be that obtained by application of the theoretical corrections. The fact that (except for the values at $\frac{x}{c} = 0.075$ already assumed to be in error) the M_l-distributions of these tests for the open and closed jets have essentially the same shape for the same value of M_a up to a value of 0.700 (near the critical value) suggests that correction should be possible. At the choking Mach number in the closed jet $M_a = 0.797$, however, the distribution of M_l is already considerably different from that at the same Mach number in the open jet and approaches more nearly the M_l-distribution of the open jet for $M_a = 0.900$; but even for the choking Mach number, so far as can be judged from figure 8, coincidence with an M_l-distribution for an open jet might occur at some value of M_a somewhat less than 0.900 and correction might still be possible. The compressibility effect on the interference is shown in the increasing spread at given values of M_a between the local Mach number distributions for open and closed jets.

Correction was first made for wake constriction and uniform pressure gradient by use of the theory previously discussed by correcting the stream Mach number to

$$M_{av} = \frac{M_a + M_b}{2}$$

Local Mach number distributions M_l at chosen values of M_{av} are shown in figure 9. The M_l-values of figure 9 for the closed jet are the same as those of figure 8; only the stream Mach numbers have been changed from M_a to M_{av}. From figure 9 the correction for wake constriction and pressure gradient can be seen to bring the Mach number distributions for open and closed jets into much closer agreement, particularly at the lower Mach numbers, than if this correction had not been applied.

The relation between M_a and M_b is shown in figure 10. For both open and closed jets, M_b is greater than M_a but the difference between the two is much greater for the closed jet than for the open jet. This effect agrees qualitatively with the wake-constriction theory (see equations (15) and (16) and the discussion following these equations). At moderate Mach numbers for which an estimate of the wake constriction can reasonably be made, however, the corrections, particularly for the closed jet, are much greater than indicated by the wake-constriction theory. For the closed jet, for example, the corrections are about five times as great at $M_a = 0.600$, which indicates a pressure gradient in the tunnel.

Local Mach number distributions at values of the stream Mach number corrected for solid constriction as well as for wake constriction and pressure gradient are shown in figure 11. The distributions of M_l for the closed jet are the same as those given in figure 9, but the stream Mach numbers M_{av} have been corrected to M_{corr} by adding the solid-constriction correction for closed-throat tunnels given by equations (30) and (31). For the open jet the values of M_a corresponding to the values of M_{corr} for the closed-throat tunnel have been found by subtracting from the values of M_{corr} for the closed-throat tunnel the solid-constriction correction (equations (30) and (31)) and the wake-constriction and pressure-gradient correction $\frac{M_b - M_a}{2}$. At values of M_a so obtained, the M_l-values for use in figure 11 were taken from the plots of M_l against M_a for the open-jet tests. Additional distributions of M_l are shown in figure 11 for a Mach number M_{corr} of 0.790, which is greater than the critical value and corresponds to a Mach number M_a of 0.750 in the closed jet. The Mach number value M_{corr} represents the stream Mach number completely corrected theoretically except for the small direct influence of the airfoil profile at the measuring orifices. (See equation (13).) This influence is the same in both open and closed jets and therefore does not affect the comparison.

Fair agreement is obtained between Mach number distributions for the open and closed jets at the same values

of the corrected Mach number M_{corr} except at the Mach number corresponding to choking in the closed tunnel. The accuracy of the data is not such as to permit the theoretical wind-tunnel corrections to be checked; the most that can be said is that, when the theoretical corrections were applied, the Mach number distributions up to a stream Mach number between the critical and the choking value for the closed jet came into approximate agreement and that the agreement was better even at the choking Mach number than if no correction had been applied.

In order to investigate the type of flow existing for these tests, the Mach number distribution in potential flow was computed at a free-stream Mach number of 0.405 and is shown in figure 11. In calculating this Mach number distribution, the velocity distribution for incompressible flow $\left(V_l/V_o\right)_i$ was obtained by the method of reference 9. The induced-velocity coefficient corresponding to this velocity distribution,

$$\left(\frac{\Delta V_l}{V_o}\right)_i = \left(\frac{V_l}{V_o}\right)_i - 1$$

was then multiplied by the factor $\frac{1}{\sqrt{1 - M^2}}$ (see reference 10) to give the induced velocity at a stream Mach number of 0.405; that is,

$$\left(\frac{\Delta V_l}{V_o}\right)_c = \left(\frac{\Delta V_l}{V_o}\right)_i \times \frac{1}{\sqrt{1 - (0.405)^2}}$$

The stream velocity corresponding to this induced-velocity ratio at the Mach number 0.405 is

$$\left(\frac{V_l}{V_o}\right)_c = \left(\frac{\Delta V_l}{V_o}\right)_c + 1$$

and the Mach number distribution is obtained from the isentropic flow relation

$$\frac{M_l}{M_o} = \frac{V_l/V_o}{\sqrt{1 - \frac{\gamma - 1}{2} M_o^2 \left[\left(\frac{V_l}{V_o}\right)^2 - 1\right]}} \tag{33}$$

Except for the erroneous values at $\frac{x}{c} = 0.075$ for the closed tunnel, the agreement between the calculated Mach numbers and the corrected measured values is reasonably good and indicates that, in spite of the small size of the model, no serious flow separation occurred and the Reynolds number was therefore not below the critical value.

The method of applying the corrections may be clarified by reference to figures 12 to 14. In these figures, the local values of the Mach number M_l at the 27.5-percent-chord station are divided by M_a, M_{av}, and M_{corr} in turn and plotted against M_a, M_{av}, and M_{corr}, respectively.

The process of correction of two Mach number ratios in the open and closed jets is shown in figure 14. The local Mach numbers M_l were obtained correctly from the local pressures p_l and the total pressures H by use of equation (1). Consider the value of M_l/M_{corr} for the closed-throat tunnel plotted at $M_{corr} = 0.775$ in figure 14. The corresponding value of M_l was originally divided by M_a (= 0.749) and plotted at $M_a = 0.749$ in figure 12. Correction for pressure gradient and wake effect gave a value of M_{av} of 0.766. The value of M_l was therefore divided by M_{av} (= 0.766) and this ratio was plotted at $M_{av} = 0.766$ in figure 13. The correction involved a decrease of the Mach number ratio from 1.439 to 1.407 and an increase of the Mach number at which the local Mach number ratio was plotted from 0.749 to 0.766. The solid-constriction correction involved an additional increment of Mach number of 0.009.

The value of M_l was therefore divided by M_{corr} (= 0.775) and the ratio was plotted at $M_{corr} = 0.775$ in figure 14. The values of the Mach number ratios for the open-throat tunnel were corrected in the same way but in this case the solid-constriction correction was opposite in sign to that due to the wake and pressure gradient. For this reason, the point in figure 14 for the open jet at $M_{corr} = 0.790$, for instance, is almost the same as the corresponding uncorrected point in figure 12.

In figure 14 the open-jet values of the local Mach number ratio for M_{corr} greater than $M_{corr} = 0.900$ have been omitted because at these high Mach numbers the theoretical compressibility effect on the solid-constriction corrections is held in doubt and no closed-jet values are available for comparison. The highest corrected stream Mach number for the closed jet is 0.858, which corresponds to tunnel choking. The corrected Mach number ratio for the closed-throat tunnel at this station (27.5 percent chord) and at this stream Mach number falls below the corrected open-jet value, whereas with the same corrected stream Mach number but at stations farther back on the surface (fig. 11) the Mach number ratios for the closed jet considerably exceed the open-jet values. This behavior suggests that tunnel-wall-interference investigations based on isolated pressures on the model rather than on pressure distributions are not to be relied upon.

Schlieren photographs.- Additional information on the nature of the boundary interference and flow in open-throat and closed-throat tunnels can be obtained from the schlieren photographs of figures 5 and 6. Up to the Mach number at which shock waves first occur (figs. 5(a) to 5(c) and 6(a) to 6(d)), the flow in the vicinity of the model appears the same in both open and closed jets. At somewhat higher Mach numbers (figs. 6(g) to 6(t)), disturbances in the open jet changed the flow pattern near the model and thereby prevented an accurate comparison between the flow patterns in the open and closed jets. In view of the unsteadiness in the flow, which at times caused the flow about the airfoil to be asymmetrical, the approximate agreement between the corrected Mach number distributions for open and closed jets is rather surprising and is perhaps fortuitous. Nevertheless, even the flow patterns show certain similarities.

The critical Mach number M_{cr} was judged from sharp prints to correspond to a Mach number M_a in the closed tunnel of 0.717, which with corrections would be only slightly more than the theoretical value of M_{cr} of 0.720. Unfortunately, because of the necessity of changing the tunnel walls for the schlieren setup, accurate wall-interference corrections cannot be applied. The critical Mach number itself cannot be accurately defined, however, because the first gathering of the shock wave by which the critical Mach number is determined is a gradual process and does not occur suddenly at one specific value of the stream Mach number. It is evident from figure 6(e), although the flow is unsymmetrical, that the critical Mach number in the open jet is close to 0.728; no great difference therefore exists between the critical Mach numbers in open and closed jets.

At Mach numbers between the critical and about 0.75 or 0.76 (figs. 5(d), 5(e), 6(f), and 6(g)), the results for open and closed jets agree in showing no large disturbances in the flow, though the intensity of the shocks increases. At still higher Mach numbers (figs. 5(f) to 5(m) and 6(h) to 6(p)), both open-jet and closed-jet tests show increasing intensity of shock and separation of the flow with development of a wide wake. The shock patterns are somewhat similar but, as the theory would lead one to expect, the shock waves develop toward the wall in the closed jet as the Mach number is increased, whereas in the open jet the ends of the shock waves remain diffuse. Even at the choking Mach number for the closed jet (figs. 5(n) and 5(o)), open-jet flows can be found with similar shock patterns on the airfoil (figs. 6(s) and 6(t)), though the pressure distributions (figs. 3 and 4) in the Mach number ranges at which these two sets of schlieren pictures were made do not agree. When the tunnel power in the closed jet is increased beyond the smallest amount necessary for choking (fig. 5(p)), the shock pattern is different from any obtained for the open jet.

Conditions near Choking

The choking Mach number for the closed tunnel $M_{a_{ch}}$ for the present tests is compared in figure 15 with the choking Mach numbers obtained in two other tunnels and with the theoretical values of choking Mach number

obtained from equation (32) without consideration of boundary-layer effects. The value of the choking Mach number for the present tests falls above the theoretical curve, whereas from purely potential-flow theory it should fall on or below the theoretical curve. If allowance were made for the pressure gradient existing in the tunnel (that is, if the tunnel velocity had been obtained from a tunnel calibration), moreover, the choking Mach number would fall still farther above the theoretical value. The fact that the tunnel chokes at a Mach number greater than the theoretical value is believed to be due to the decrease in thickness of the wall boundary layer in regions of increasing velocity as discussed with relation to equation (32). The required gradient obviously exists on the side walls in the vicinity of the model and is known to extend to the upper and lower boundaries as the Mach number approaches the choking value. The negative density gradient corresponding to the negative pressure gradient is shown by the dark regions above and below the model in figures 5(o) and 5(p) and is seen to cover the whole cross section of the tunnel. The thinning of the wall boundary layer causes the effective cross sections at the model to be larger than would otherwise be the case so that a greater mass flow passes than is assumed in the theory, which causes the upstream Mach number where the boundary layer is relatively unaffected to be higher than it would otherwise be.

Further evidence to support the argument advanced herein with regard to the effect of the boundary layer is contained in the relative positions of the points in figure 15. Both the Langley rectangular high-speed tunnel and the tunnel used for the present tests have narrow rectangular cross sections in contrast to the approximately circular section of the Langley 24-inch high-speed tunnel. The ratio of boundary area per unit length to cross-sectional area is therefore much greater for these rectangular tunnels than for the almost circular tunnel and the boundary-layer effects considered should also be greater. The expected effect is indicated in figure 15 by the fact that except for one single point the values for the rectangular tunnels fall near the theoretical curve, whereas all values from the almost circular tunnel fall below the curve. Of course, the influence of the model, which should tend to cause the experimental points to fall below the theoretical curve, would also make itself felt; and, the model influence would be greater the larger the model. This effect

appears at the higher $\frac{t}{h}$-values in figure 15. The wall boundary layer must affect the flow in such a way as to alleviate the tunnel constriction at all Mach numbers, but the effect rapidly increases as the Mach number approaches the choking value.

The shock extends to the wall at the choking Mach number (figs. 5(n) and 5(o)), which shows that sonic speed must also extend to the wall, so that theoretically no further increase in mass flow with the same upstream stop pressure and temperature is possible. In figure 5(p) an increase in tunnel power has thus produced a change in the shock pattern without a change in the upstream Mach number. As shown in figure 16, the pressure difference between upstream and downstream pressure orifices is also increased without a change in upstream Mach number. Indeed, the reduction in back pressure behind the shock (or the increase of pressure ahead of the shock) is the cause of the change of the shock-wave pattern.

The pressure difference between upstream and downstream orifices evidently begins to increase rapidly (see fig. 16) at a speed somewhat above the critical speed and apparently this increase might be used to determine the highest Mach number for which the test results obtained could be considered reliable. In the open jet, as may be seen from figure 16, no large pressure difference such as occurs in the closed jet exists.

Change of Velocity Ratio $\frac{V_l}{V_o}$ with Mach Number

The existence of corrected experimental velocity ratios affords an opportunity for comparing with experiment several formulas for the compressibility effect on the local velocities. Four of the best known of these formulas are

(1) A relation corresponding to the Prandtl-Glauert theory (references 10 and 11)

$$\left(\frac{V_l}{V_o}\right)_c = 1 + \frac{\left(\frac{V_l}{V_o}\right)_i - 1}{\sqrt{1 - M_o^2}} \qquad (34)$$

(2) The Kármán-Tsien relation (from equation (61) of reference 12)

$$\left(\frac{V_l}{V_o}\right)_c = \left(\frac{V_l}{V_o}\right)_i \frac{1 - \left(\frac{M_o}{1 + \sqrt{1 - M_o^2}}\right)^2}{1 - \left(\frac{M_o}{1 + \sqrt{1 - M_o^2}}\right)^2 \left(\frac{V_l}{V_o}\right)_i^2} \tag{35}$$

(3) The Temple-Yarwood relation (from equation (51) of reference 13)

$$\left(\frac{V_l}{V_o}\right)_c = \left(\frac{V_l}{V_o}\right)_i 3\left(1 - \frac{5}{4}\tau_1\right) \frac{\cos \frac{1}{3}(\pi + \sigma)}{\cos \sigma} \tag{36}$$

where

$$\tau_1 = \frac{M_o^2}{5 + M_o^2}$$

and

$$\cos \sigma = \frac{3\sqrt{3}}{2}\left(1 - \frac{5}{4}\tau_1\right)\left(\frac{5}{4}\tau_1\right)^{1/2}\left(\frac{V_l}{V_o}\right)_i$$

(4) The results of Kaplan's application to a bump and to a curved surface (see pages 16 and 17 of reference 14) of the extended theory of compressible flow with small perturbations.

The comparison of the experimental and theoretical variation of velocity ratio V_l/V_{eff} with Mach number M_{eff} is shown in figure 17 for values at the 27.5-percent-chord station. In this figure, the correction for the

direct influence of the profile at the calibration orifices has been applied (equation (13)) in addition to the other corrections to give effective values of the stream velocity and Mach number, V_{eff} and M_{eff}. The theoretical curves were passed through a value of M_{eff} of 0.4, which was determined by fairing through the closed-jet values of V_l/V_{eff} in this region.

The simple Kármán-Tsien relation (equation (35)) is seen from figure 17 to agree with the experimental variation of V_l/V_{eff} at the 27.5-percent-chord station as well as any of the theoretical variations tried. According to the theory, these theoretical relations are expected to describe the experimental variation best near the peak velocity. In the present tests, the Kármán-Tsien relation was also found approximately to describe the change of V_l/V_{eff} with Mach number, up to Mach number values somewhat beyond the critical, at points farther back on the airfoil. This approximate agreement of the Kármán-Tsien relation with experiment is consistent with past experience and suggests, especially inasmuch as the relation is also relatively simple, that this relation should be used to extrapolate low-speed velocity and pressure coefficients to high speed, at least for values of these coefficients in the vicinity of and for moderate values of the peak velocity. No theory, based on potential flow, should of course be expected to hold in regions in which the flow departs considerably from the potential.

INTERPRETATION OF RESULTS AND CONCLUSIONS

From the foregoing analysis of two-dimensional tests of the NACA 0012 airfoil of 1-inch chord in 3-inch open and closed jets, the following remarks are considered to be justified:

1. In applying tunnel-wall corrections, care must be exercised to take account of any interference at the orifices used in determining the tunnel velocity as well as to obtain a correct empty-tunnel calibration.

2. The corrections for wake and solid constriction were found to be sufficient up to a Mach number between the critical and choking values to bring the results for

the open and closed jets into approximate agreement. The accuracy was insufficient, however, to prove the exactness of the corrections.

3. In the closed-throat tunnel the speed is limited by choking, which is the most severe effect of the tunnel walls. Even at a velocity very close to that at the first attainment of choking, however, an open-jet Mach number distribution (one occurring at an uncorrected stream Mach number less than unity) could be found which was not greatly different from that obtained in the closed jet though the corresponding apparent stream Mach numbers were greatly different. Application of the theoretical corrections employed in this report failed to bring the results for the open and closed jets at the corrected velocity for the choking Mach number in the closed jet into coincidence. With the approach of choking, correction by any method may be impossible.

4. If, after the choking Mach number is reached, the tunnel power is increased, the pressure difference between points upstream and downstream from the model is increased without any significant increase in the upstream Mach number. Inasmuch as a given Mach number upstream therefore no longer corresponds to a single pressure distribution in the tunnel, corrections are obviously impossible after the choking Mach number is reached.

5. In consideration of the severe speed limitation imposed by choking and of the large increase in tunnel-wall interference at high Mach numbers, models for high-speed tests in a closed tunnel should be much smaller than the largest models that can be successfully tested at low speeds.

6. For the open jet, the absence of choking and wake constriction and the fact that the theoretical solid-constriction corrections are relatively smaller than in a closed jet suggest that the open jet should be advantageous for tests at high Mach numbers. Certain difficulties may, however, be experienced with open tunnels. Even at low speeds the boundary conditions are only approximately satisfied by the theory and, at very high speeds (Mach number above the critical), the theoretical compressibility effects on these corrections are no longer strictly applicable. Moreover, disturbances

at the boundaries may cause the flow to be unsteady in the vicinity of the model. In order, therefore, to realize the theoretical advantages of open jets for tests at Mach numbers approaching unity, special care must be exercised to obtain a design that minimizes disturbances in the flow; large jets are expected to be advantageous in this respect. In addition, the tunnel boundary corrections up to the highest test Mach numbers must be determined with greater reliability than is now possible.

7. The methods now available for estimating corrections for tunnel-wall interference are severely limited in application. The theory is strictly applicable only in potential flow at Mach numbers less than the critical and only so long as the corrections are small. Further investigation, both theoretical and experimental, is needed to determine the nature of the corrections required, to establish the limits of practical usefulness of present methods, and to develop theory and methods of application for estimating corrections up to Mach numbers as near unity as possible and for the largest models for which corrections can be applied.

Langley Memorial Aeronautical Laboratory
National Advisory Committee for Aeronautics
Langley Field, Va., January 9, 1946

REFERENCES

1. Wood, Robert W.: Physical Optics. The Macmillan Co., 1919, pp. 94-98.

2. Glauert, H.: Wind Tunnel Interference on Wings, Bodies and Airscrews. R. & M. No. 1566, British A.R.C., 1933.

3. Allen, H. Julian, and Vincenti, Walter G.: Wall Interference in a Two-Dimensional-Flow Wind Tunnel with Consideration of the Effect of Compressibility. NACA ARR No. 4K03, 1944.

4. Fluid Motion Panel of the Aeronautical Research Committee and Others: Modern Developments in Fluid Dynamics. Vol. II, S. Goldstein, ed., The Clarendon Press (Oxford), 1938.

5. Thom, A.: Blockage Corrections and Choking in the R.A.E. High Speed Tunnel. Rep. No. Aero 1891. British R.A.E., Nov. 1943.

6. Goldstein, S.: Steady Two-Dimensional Flow past a Solid Cylinder in a Non-Uniform Stream and Two-Dimensional Wind-Tunnel Interference. R. & M. No. 1902, British A.R.C., 1942.

7. Durand, W. F.: Fluid Mechanics, Part I. Combination Fields of Flow. Vol. I of Aerodynamic Theory, div. B, ch. IV, sec. 10, W. F. Durand, ed., Julius Springer (Berlin), 1935, pp. 149-150.

8. Goldstein, S., and Young, A. D.: The Linear Perturbation Theory of Compressible Flow, with Applications to Wind-Tunnel Interference. R. & M. No. 1909, British A.R.C., 1943.

9. Theodorsen, T., and Garrick, I. E.: General Potential Theory of Arbitrary Wing Sections. NACA Rep. No. 452, 1933.

10. Prandtl, L.: General Considerations on the Flow of Compressible Fluids. NACA TM No. 805, 1936.

11. Glauert, H.: The Effect of Compressibility on the Lift of an Aerofoil. R. & M. No. 1135, British A.R.C., 1927.

12. von Kármán, Th.: Compressibility Effects in Aerodynamics. Jour. Aero. Sci., vol. 8, no. 9, July 1941, pp. 337-356.

13. Garrick, I. E., and Kaplan, Carl: On the Flow of a Compressible Fluid by the Hodograph Method. I - Unification and Extension of Present-Day Results. NACA ACR No. L4C24, 1944. (Classification changed to Restricted Oct. 1944.)

14. Kaplan, Carl: The Flow of a Compressible Fluid past a Circular Arc Profile. NACA ARR No. L4G15, 1944.

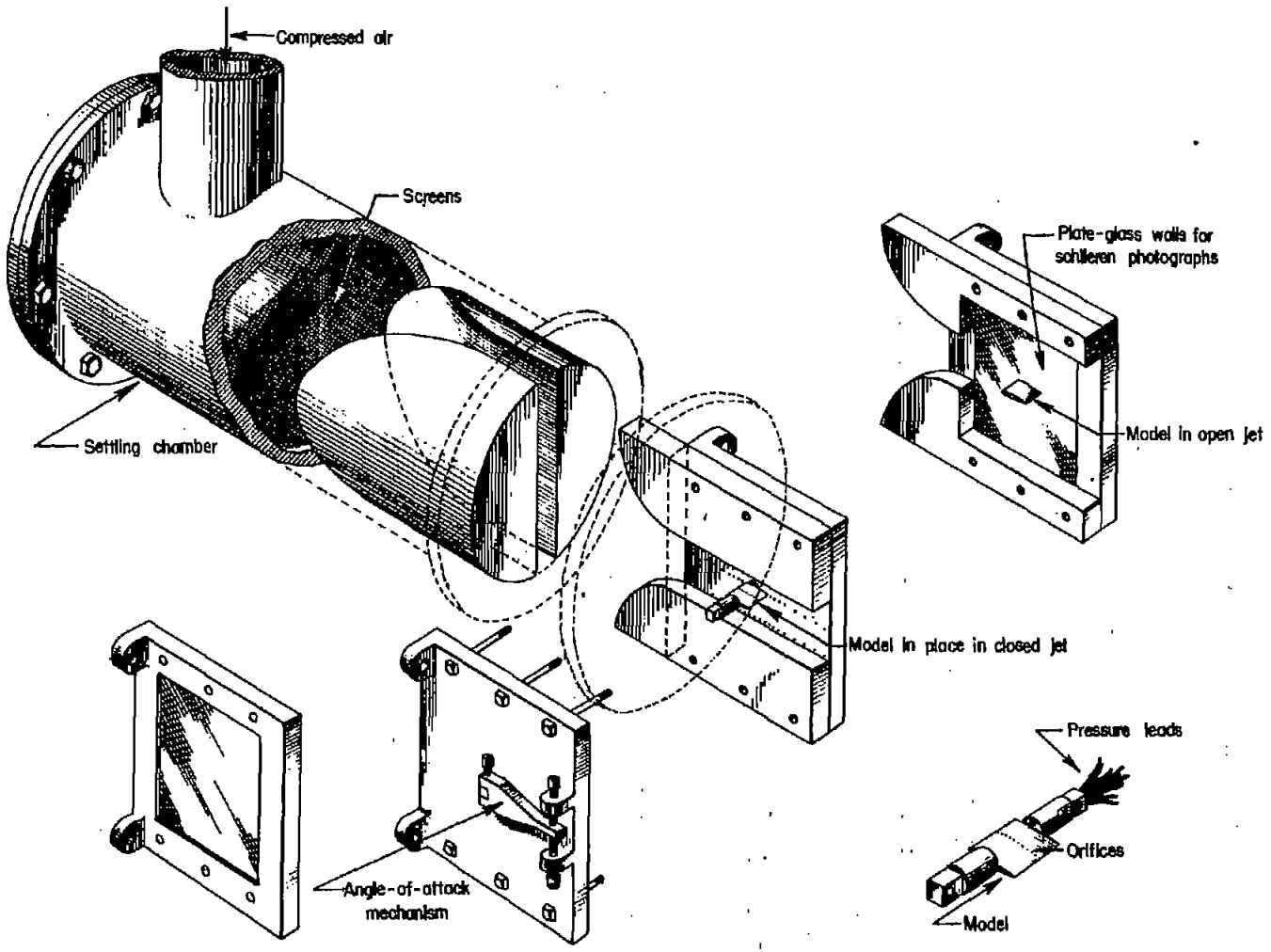

Figure 1.- Exploded view of experimental setup.

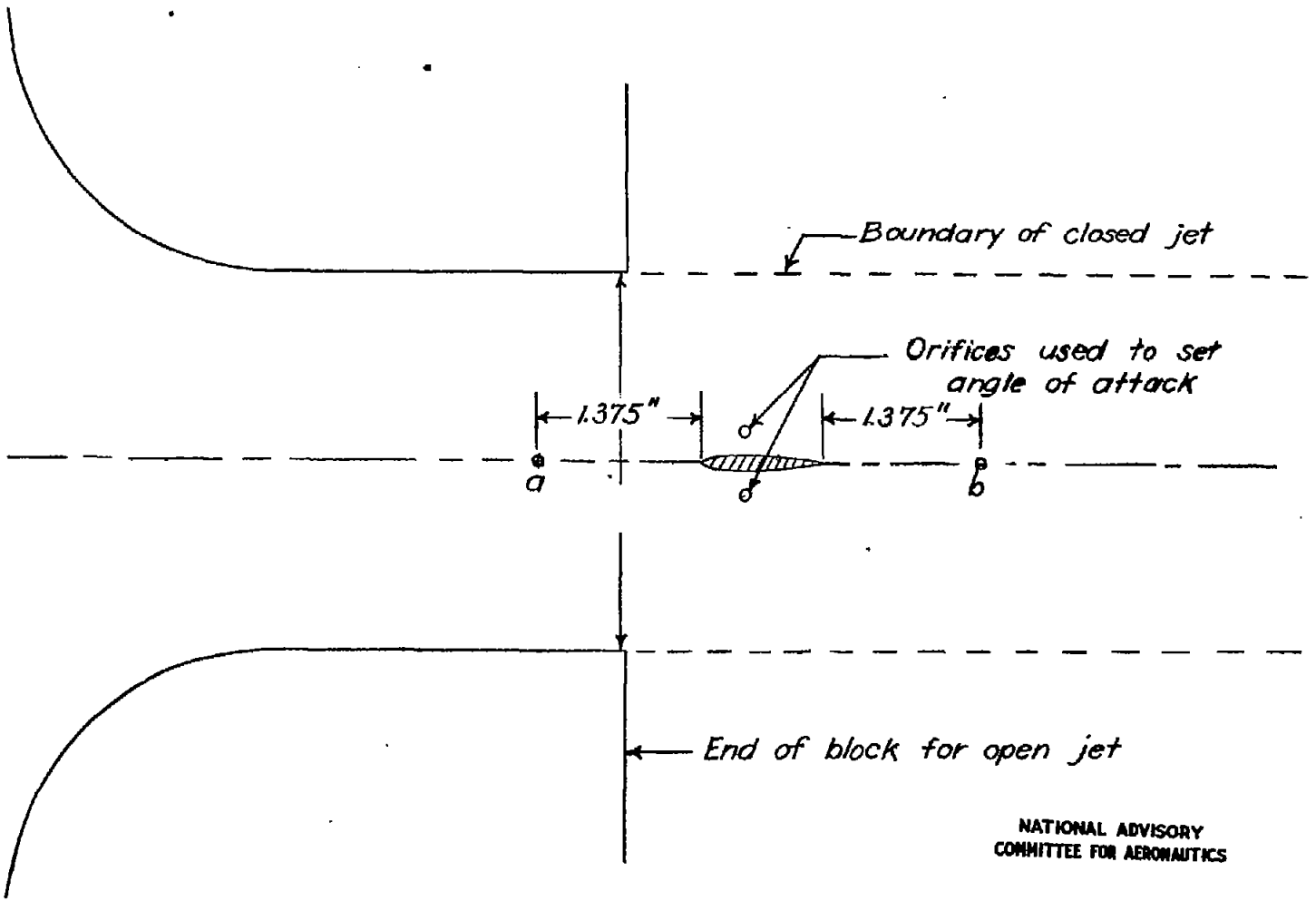

Figure 2.- Location of static-pressure orifices in wall with respect to position of airfoil model. Block simulating open jet is shown.

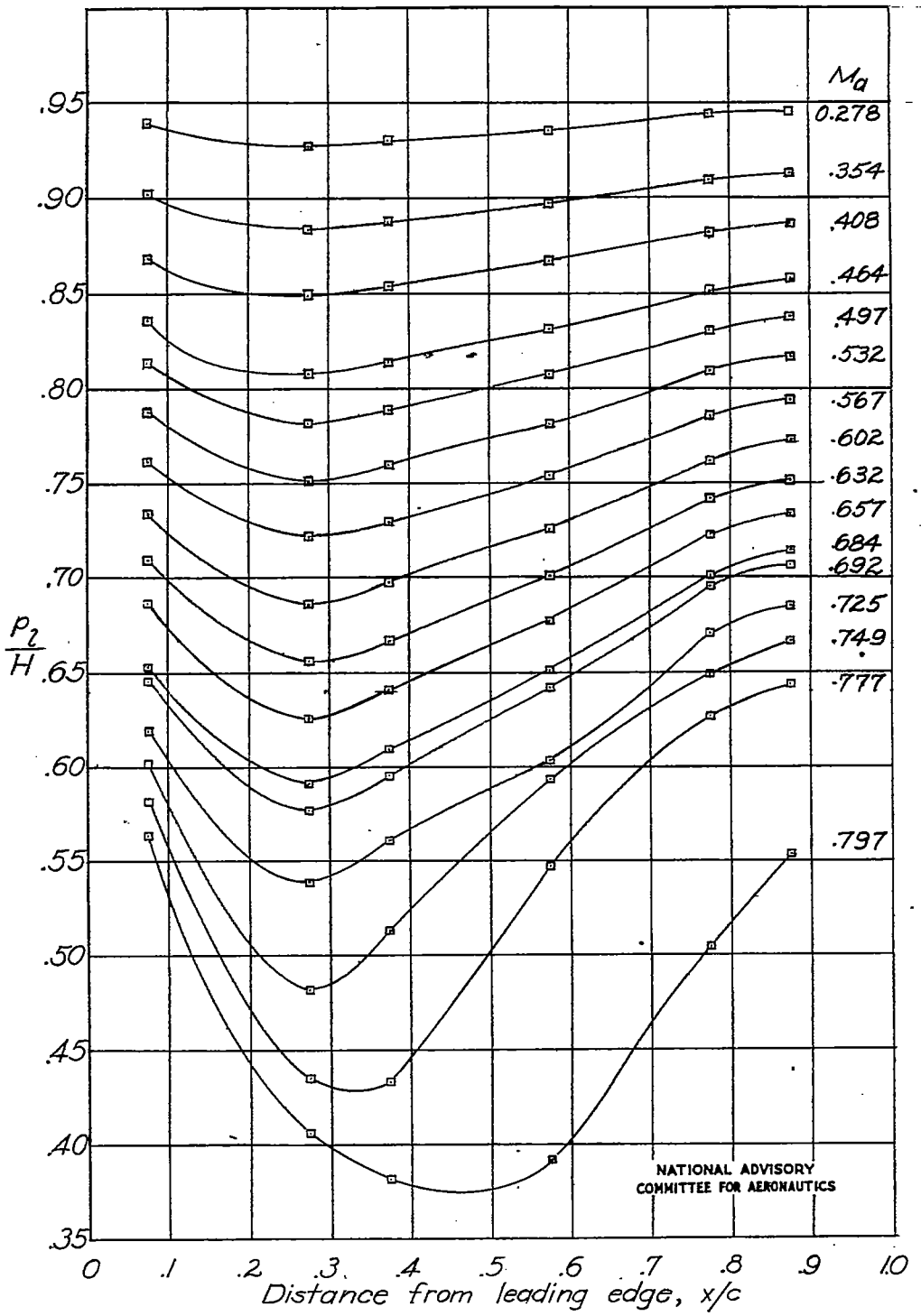

Figure 3.- Distribution of ratio of static to total pressure p_l/H about NACA 0012 airfoil of 1-inch chord in 3-inch closed jet. Mach number M_a taken at orifice 1.375 inches upstream from leading edge of model.

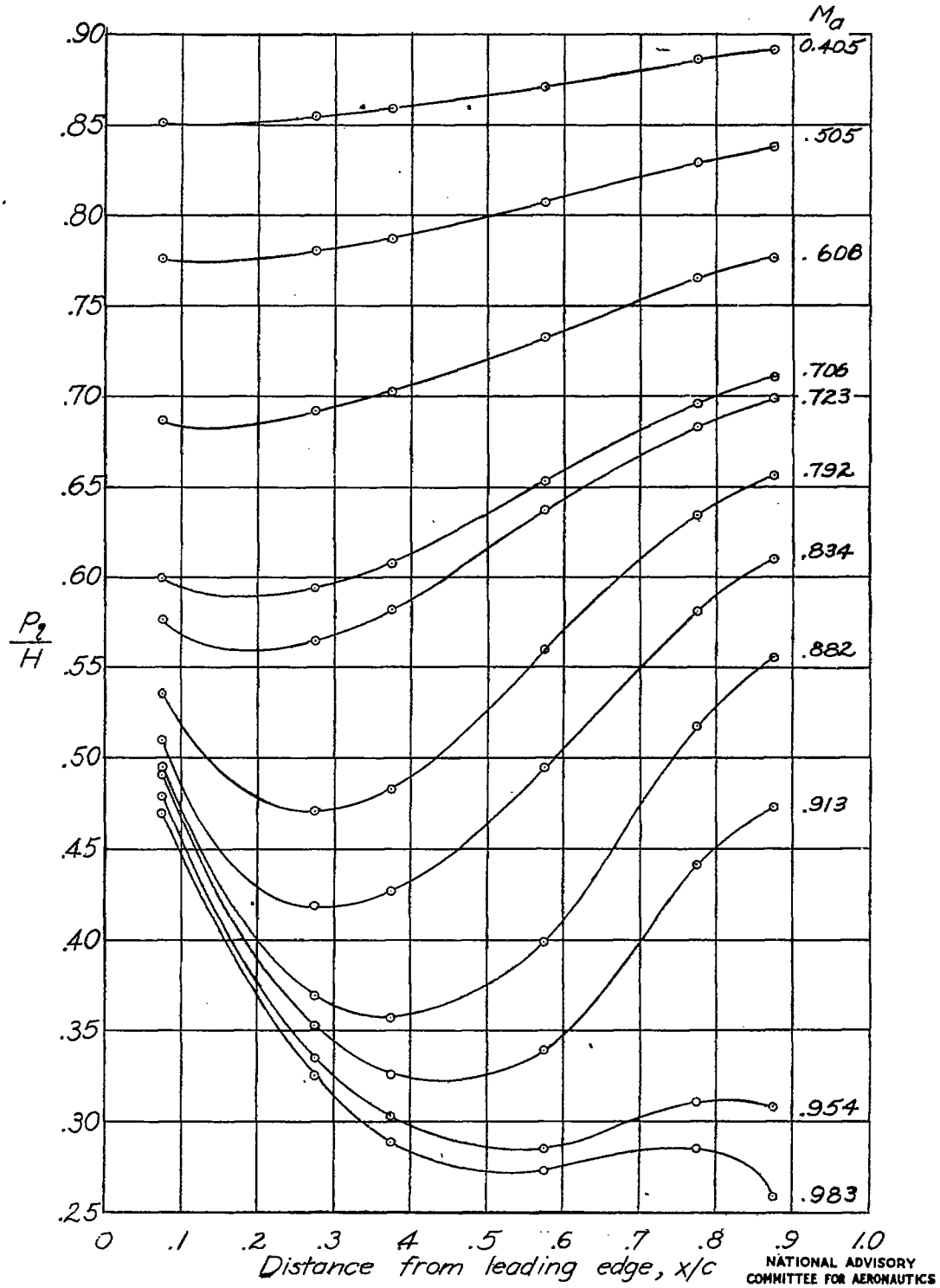

Figure 4.- Distribution of ratio of static to total pressure p_l/H about NACA 0012 airfoil of 1-inch chord in 3-inch open jet. Mach number M_a taken at orifice 1.375 inches upstream from leading edge of model.

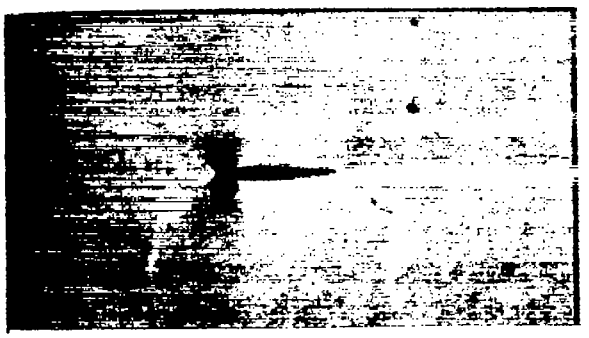

(a) M = 0.500.

(b) M = 0.664.

5.- Schlieren photographs of flow about an NACA 0012 airfoil in a closed jet. $\frac{t}{h} = 0.04$; $\alpha = 0^\circ$.

NATIONAL ADVISORY COMMITTEE FOR AERONAUTICS
LANGLEY MEMORIAL AERONAUTICAL LABORATORY - LANGLEY FIELD, VA.

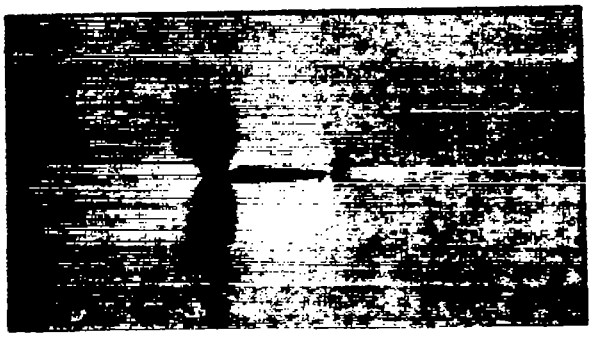

(c) M = 0.717.

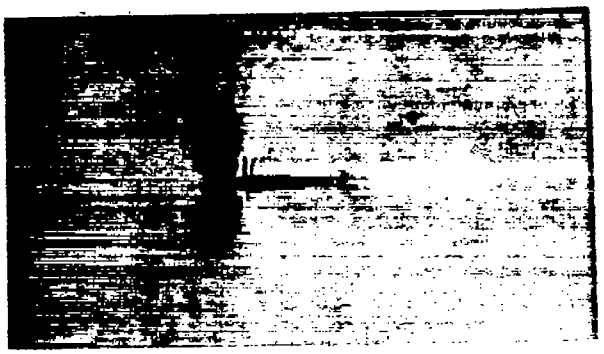

(d) M = 0.742.

Figure 5.- Continued.

NATIONAL ADVISORY COMMITTEE FOR AERONAUTICS
LANGLEY MEMORIAL AERONAUTICAL LABORATORY - LANGLEY FIELD, VA.

(e) M = 0.755.

(f) M = 0.758.

Figure 5.- Continued.

NATIONAL ADVISORY COMMITTEE FOR AERONAUTICS
LANGLEY MEMORIAL AERONAUTICAL LABORATORY - LANGLEY FIELD, VA

(g) M = 0.767.

(h) M = 0.772.

Figure 5.- Continued.

NATIONAL ADVISORY COMMITTEE FOR AERONAUTICS
LANGLEY MEMORIAL AERONAUTICAL LABORATORY - LANGLEY FIELD, VA.

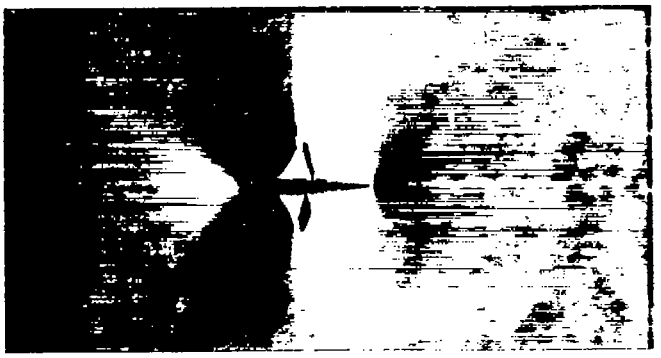

(i) M = 0.776.

(j) M = 0.780.

Figure 5.- Continued.

NATIONAL ADVISORY COMMITTEE FOR AERONAUTICS
LANGLEY MEMORIAL AERONAUTICAL LABORATORY - LANGLEY FIELD, VA.

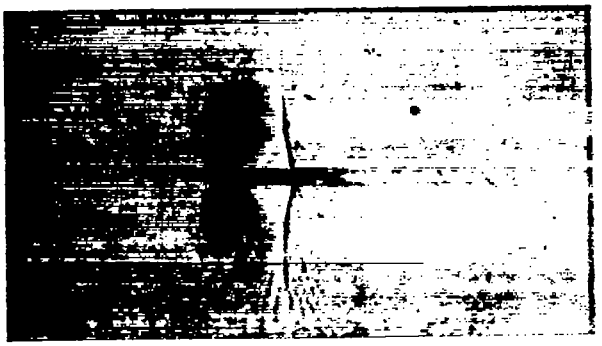

(k) M = 0.782.

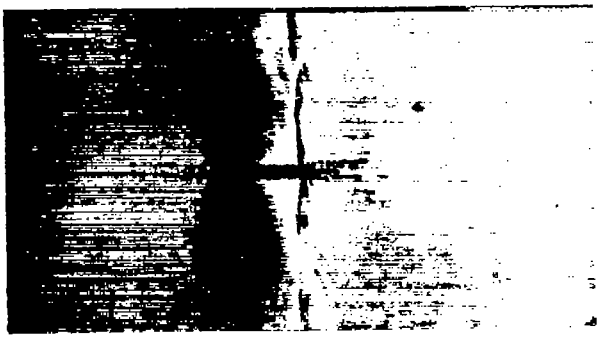

(l) M = 0.786.

Figure 5.- Continued.

NATIONAL ADVISORY COMMITTEE FOR AERONAUTICS
LANGLEY MEMORIAL AERONAUTICAL LABORATORY - LANGLEY FIELD, VA.

(m) M = 0.793.

(n) M = 0.796.

Figure 5.- Continued.

NATIONAL ADVISORY COMMITTEE FOR AERONAUTICS
LANGLEY MEMORIAL AERONAUTICAL LABORATORY - LANGLEY FIELD, VA

(o) M = 0.796.

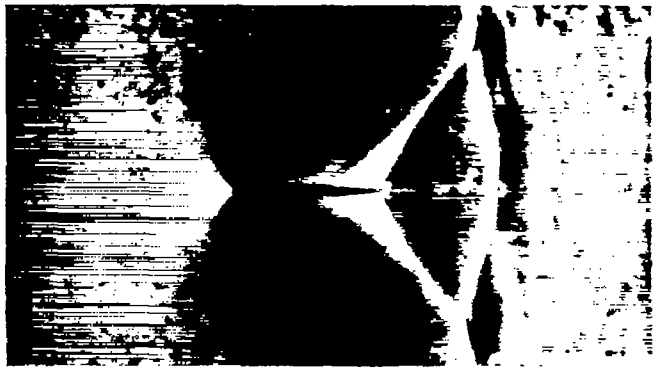

(p) M = 0.796.

Figure 5.- Concluded.

NATIONAL ADVISORY COMMITTEE FOR AERONAUTICS
LANGLEY MEMORIAL AERONAUTICAL LABORATORY - LANGLEY FIELD, VA.

(a) M = 0.652.

(b) M = 0.654.

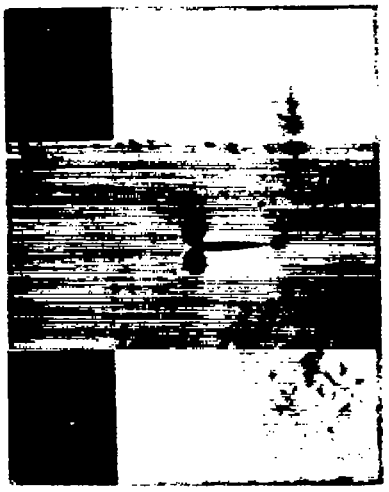

(c) M = 0.673.

(d) M = 0.673.

Figure 6.- Schlieren photographs of flow about an NACA 0012 airfoil in an open jet. $\frac{t}{h}$ = 0.04; α = 0°.

NATIONAL ADVISORY COMMITTEE FOR AERONAUTICS
LANGLEY MEMORIAL AERONAUTICAL LABORATORY - LANGLEY FIELD, VA.

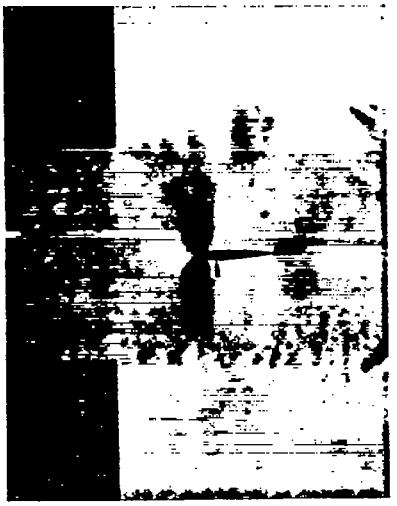

(e) M = 0.728.

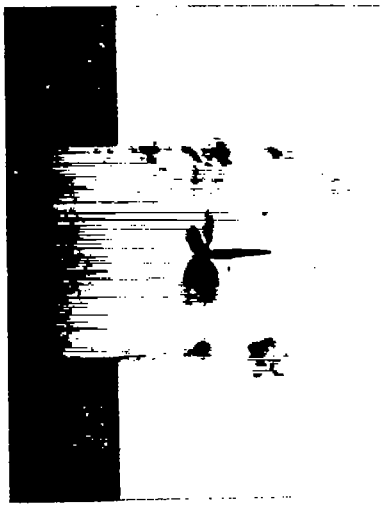

(f) M = 0.757.

(g) M = 0.758.

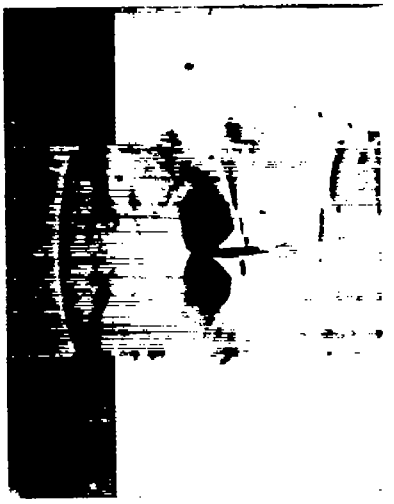

(h) M = 0.798.

Figure 6.- Continued.

NATIONAL ADVISORY COMMITTEE FOR AERONAUTICS
LANGLEY MEMORIAL AERONAUTICAL LABORATORY - LANGLEY FIELD, VA.

(i) M = 0.798.

(j) M = 0.813.

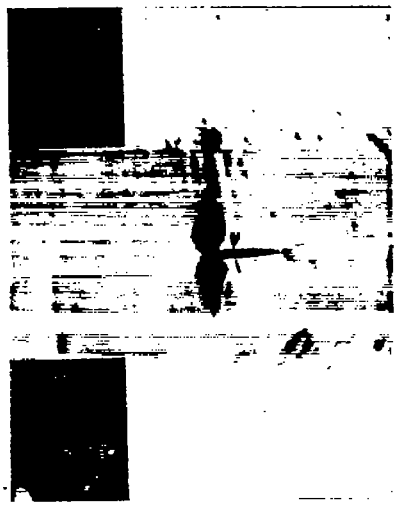

(k) M = 0.826.

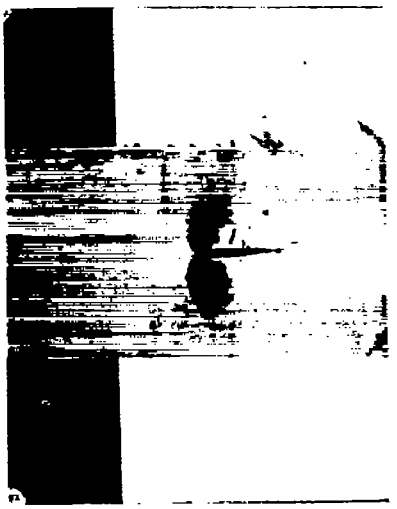

(l) M = 0.826.

Figure 6.- Continued.

NATIONAL ADVISORY COMMITTEE FOR AERONAUTICS
LANGLEY MEMORIAL AERONAUTICAL LABORATORY - LANGLEY FIELD, VA.

(m) M = 0.859.

(n) M = 0.860.

(o) M = 0.873.

(p) M = 0.873.

Figure 6.- Continued.

NATIONAL ADVISORY COMMITTEE FOR AERONAUTICS
LANGLEY MEMORIAL AERONAUTICAL LABORATORY - LANGLEY FIELD, VA.

(q) M = 0.911.

(r) M = 0.912.

(s) M = 0.964.

(t) M = 0.967.

Figure 6.- Concluded.

NATIONAL ADVISORY COMMITTEE FOR AERONAUTICS
LANGLEY MEMORIAL AERONAUTICAL LABORATORY - LANGLEY FIELD, VA.

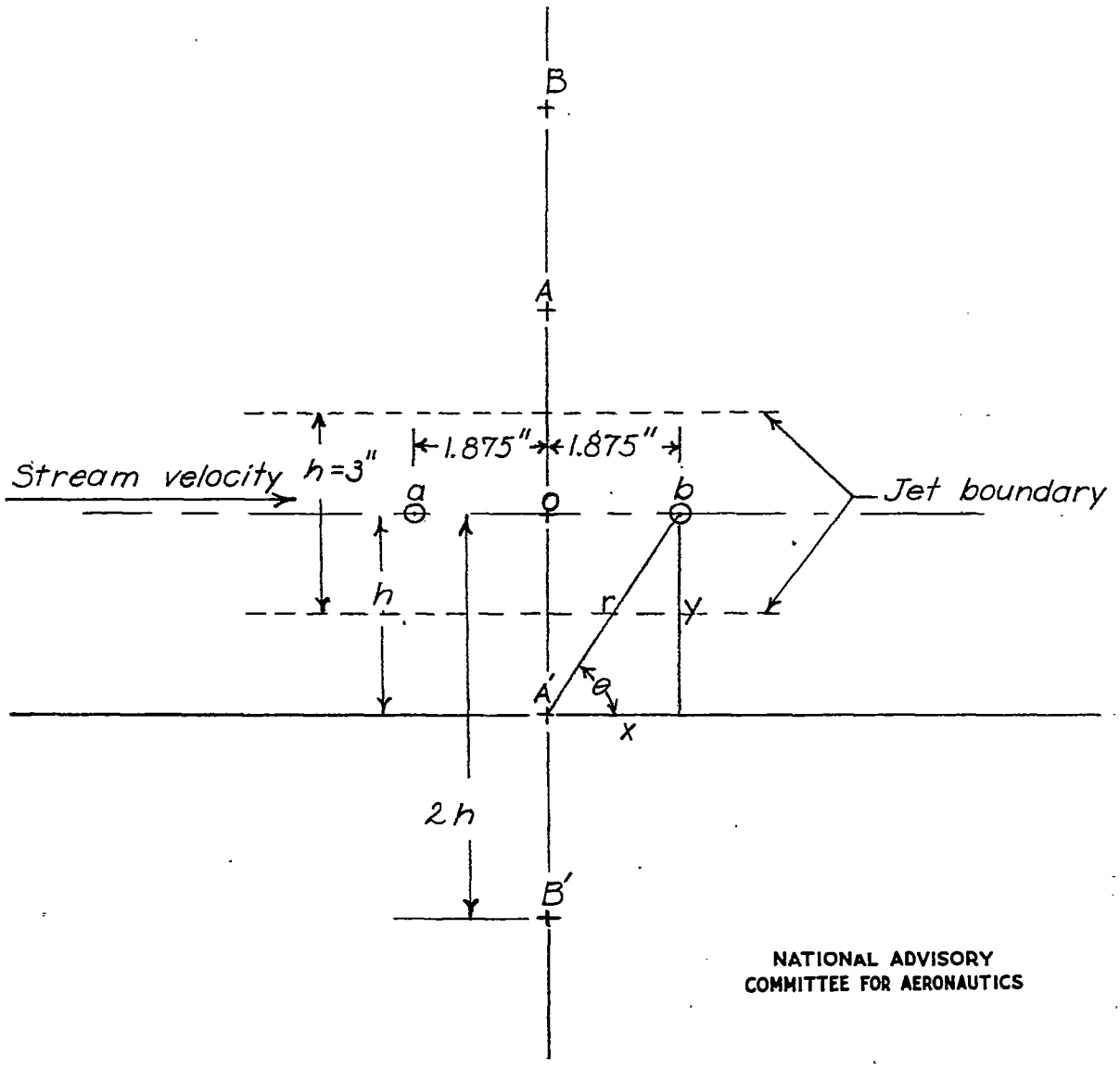

Figure 7.- Scheme for computing velocity induced at calibration orifices a and b by images A, A', B, and B'.

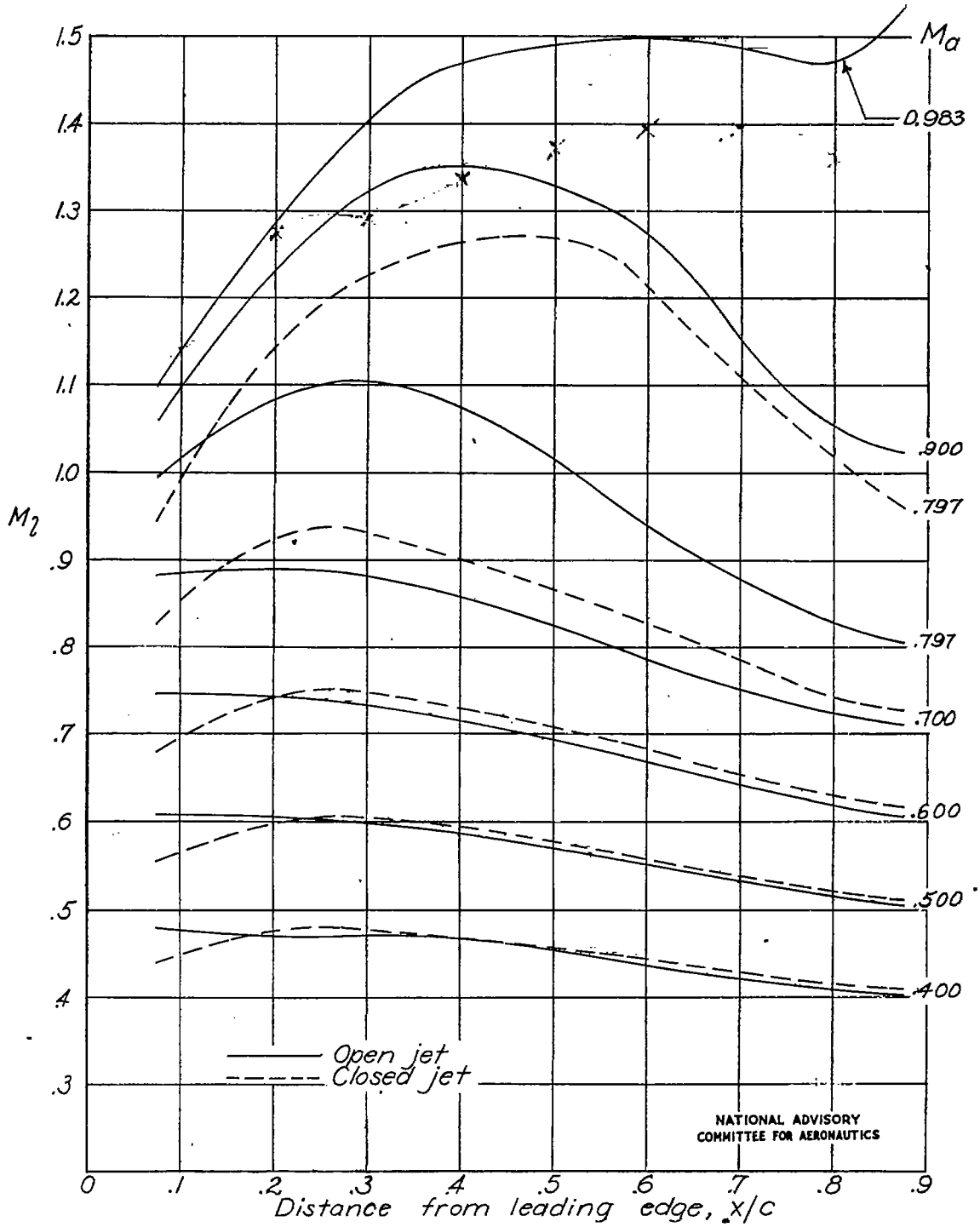

Figure 8.- Comparison of distributions of Mach number M_l over an NACA 0012 airfoil of 1-inch chord in open and closed 3-inch jets at values of the Mach number M_a taken 1.375 inches upstream from the leading edge.

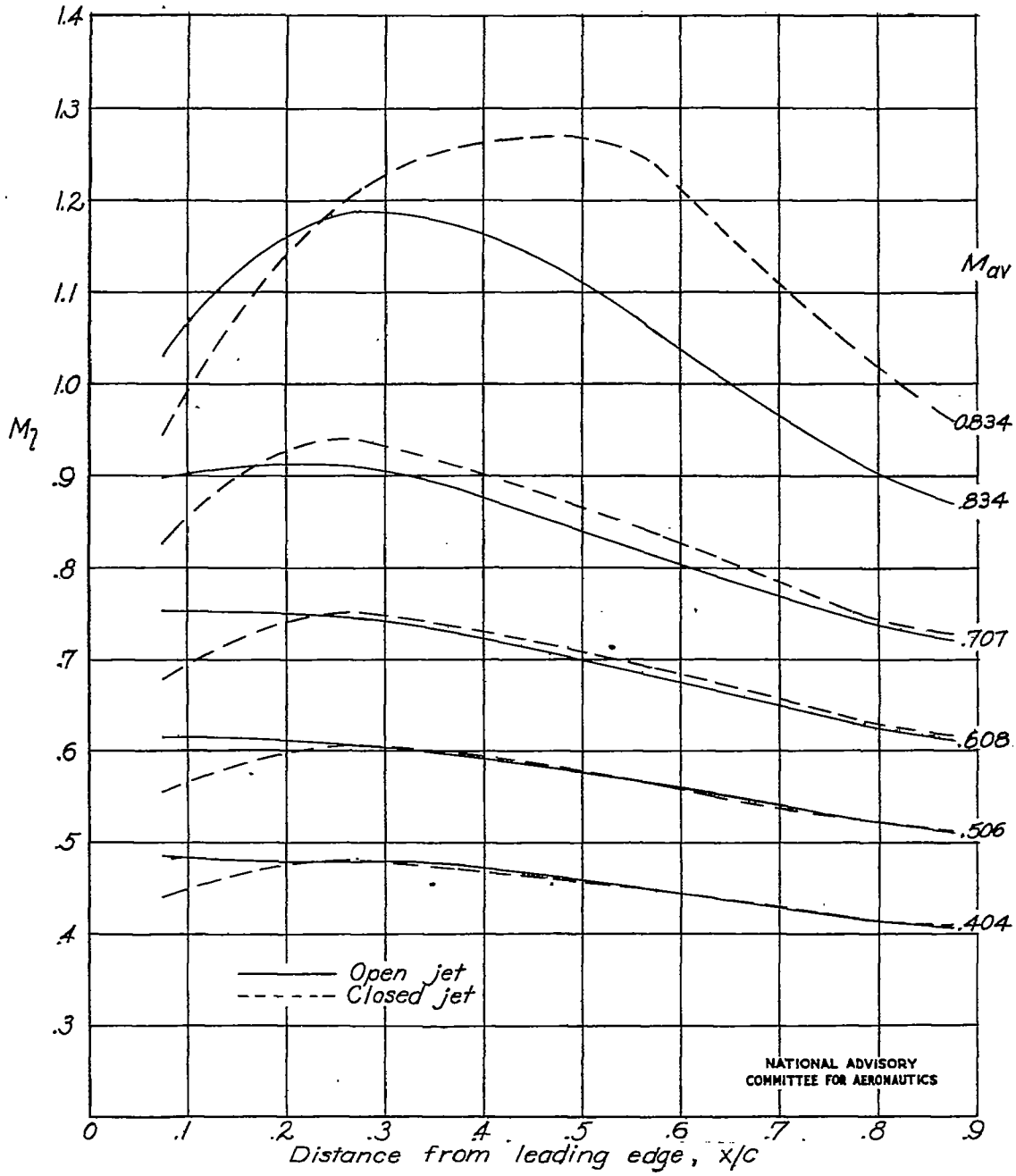

Figure 9.- Comparison of distributions of Mach number M_η over an NACA 0012 airfoil of 1-inch chord in open and closed 3-inch jets at average values of the Mach number M_{av} taken 1.375 inches upstream and downstream, respectively, from the leading and trailing edges.

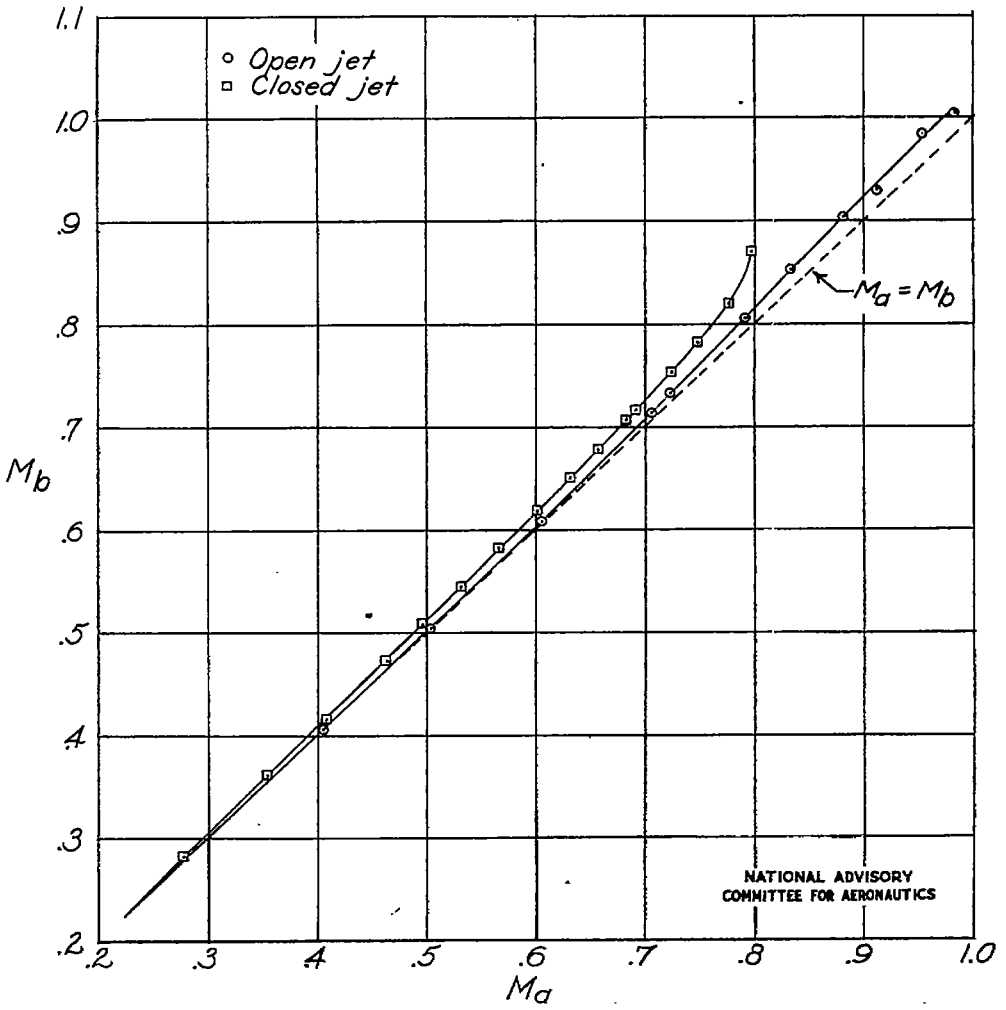

Figure 10.- Mach number M_b taken 1.375 inches downstream from the trailing edge as a function of the Mach number M_a taken 1.375 inches upstream from the leading edge of an NACA 0012 airfoil of 1-inch chord in a 3-inch jet.

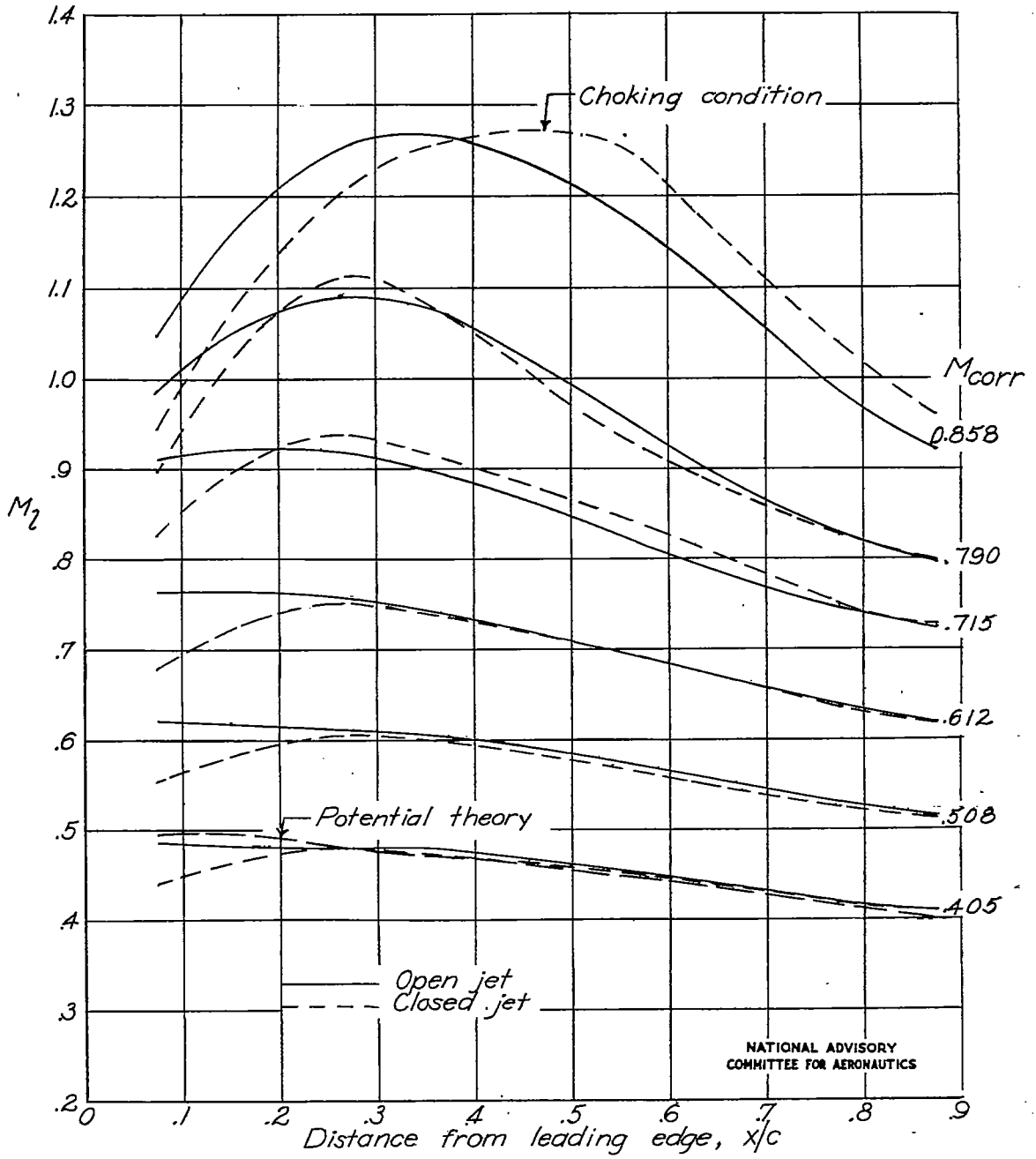

Figure 11.- Comparison of distribution of Mach number M_l over an NACA 0012 airfoil of 1-inch chord in open and closed 3-inch jets at values of the Mach number M_{corr} obtained by correcting the Mach number M_{av} for jet-boundary interference.

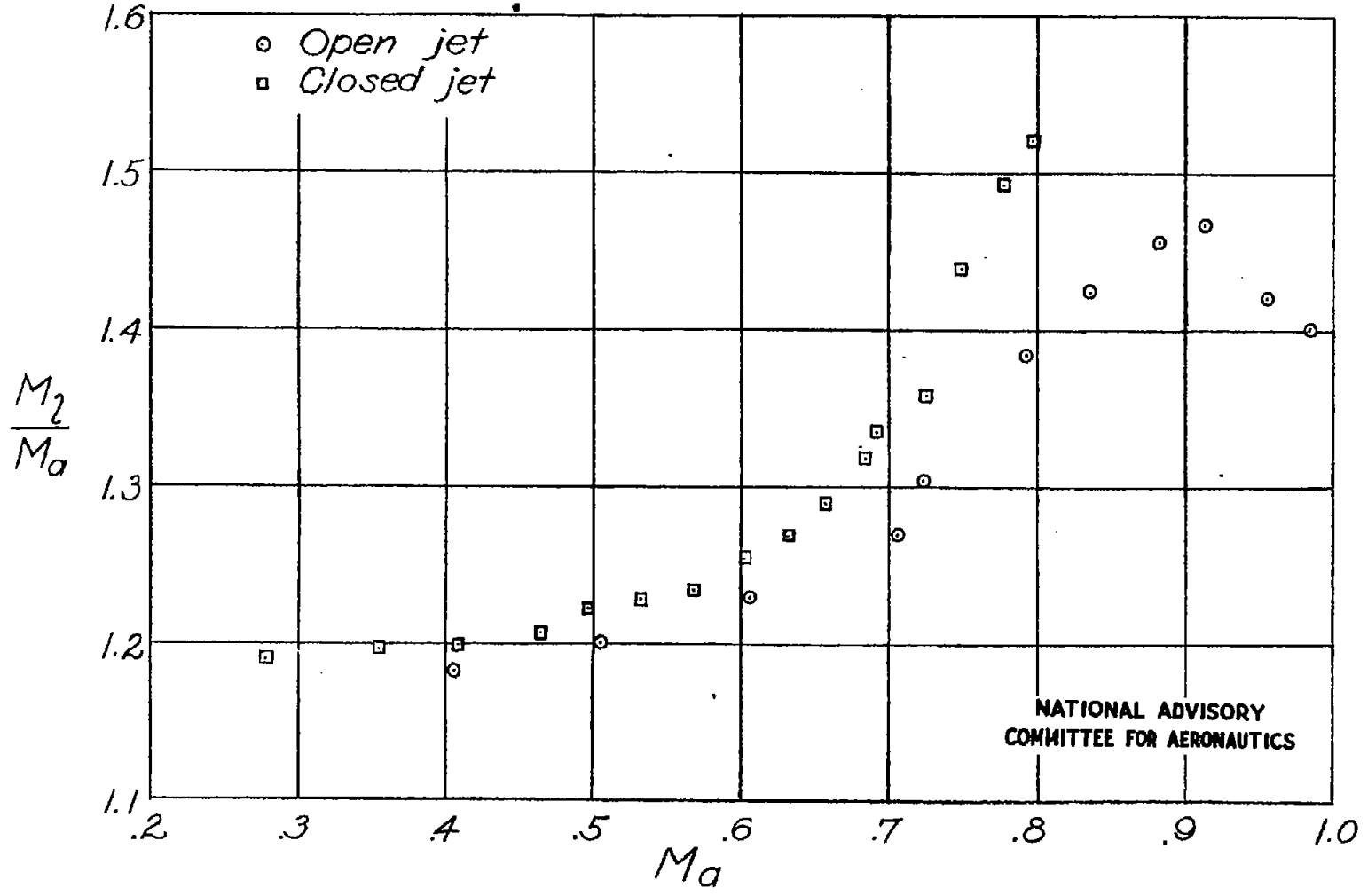

Figure 12.- Comparison of ratios of Mach number M_l at 27.5 percent chord from the leading edge to Mach number M_a taken 1.375 inches upstream from the leading edge of an NACA 0012 airfoil of 1-inch chord in open and closed 3-inch jets.

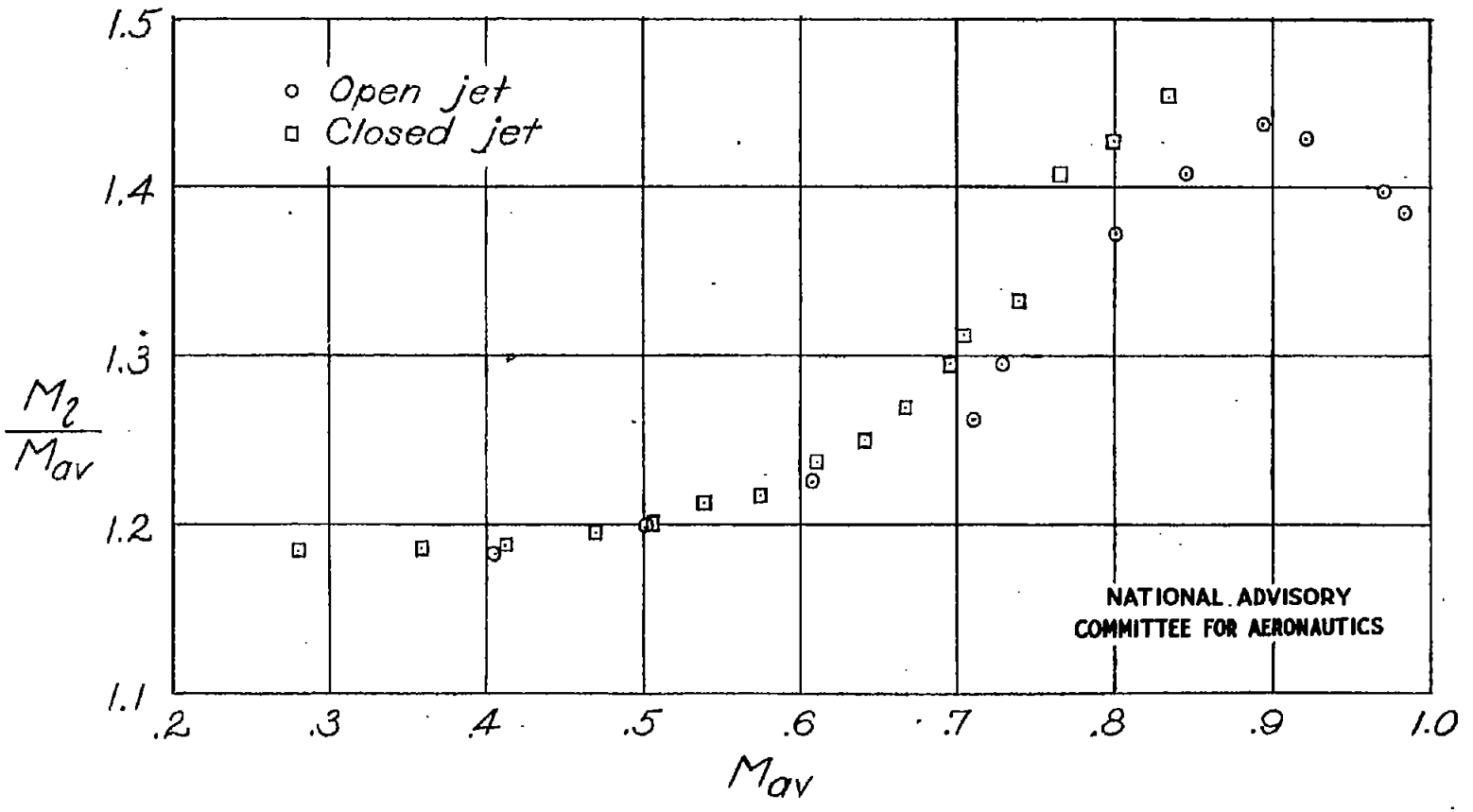

Figure 13.- Comparison of Mach number ratios M_l/M_{av} at the 27.5-percent-chord station for an NACA 0012 airfoil of 1-inch chord in 3-inch open and closed jets. M_{av} is the average value of the Mach number at points 1.375 inches upstream and downstream, respectively, from the leading and trailing edges.

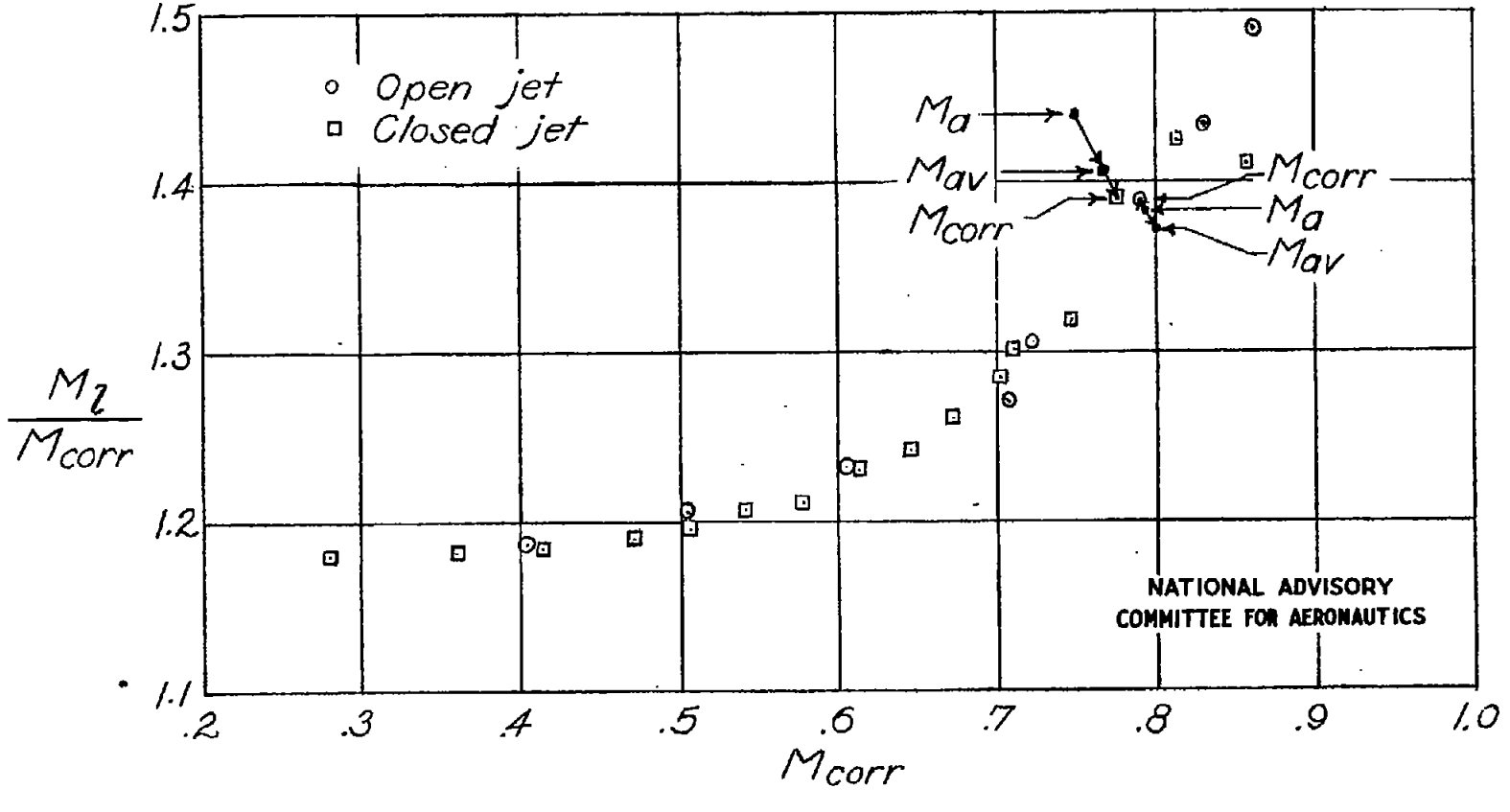

Figure 14.- Comparison of Mach number ratios M_l/M_{corr} at the 27.5-percent-chord station for an NACA 0012 airfoil of 1-inch chord in 3-inch open and closed jets. M_{corr} is obtained from M_{av} by correction for jet-boundary interference.

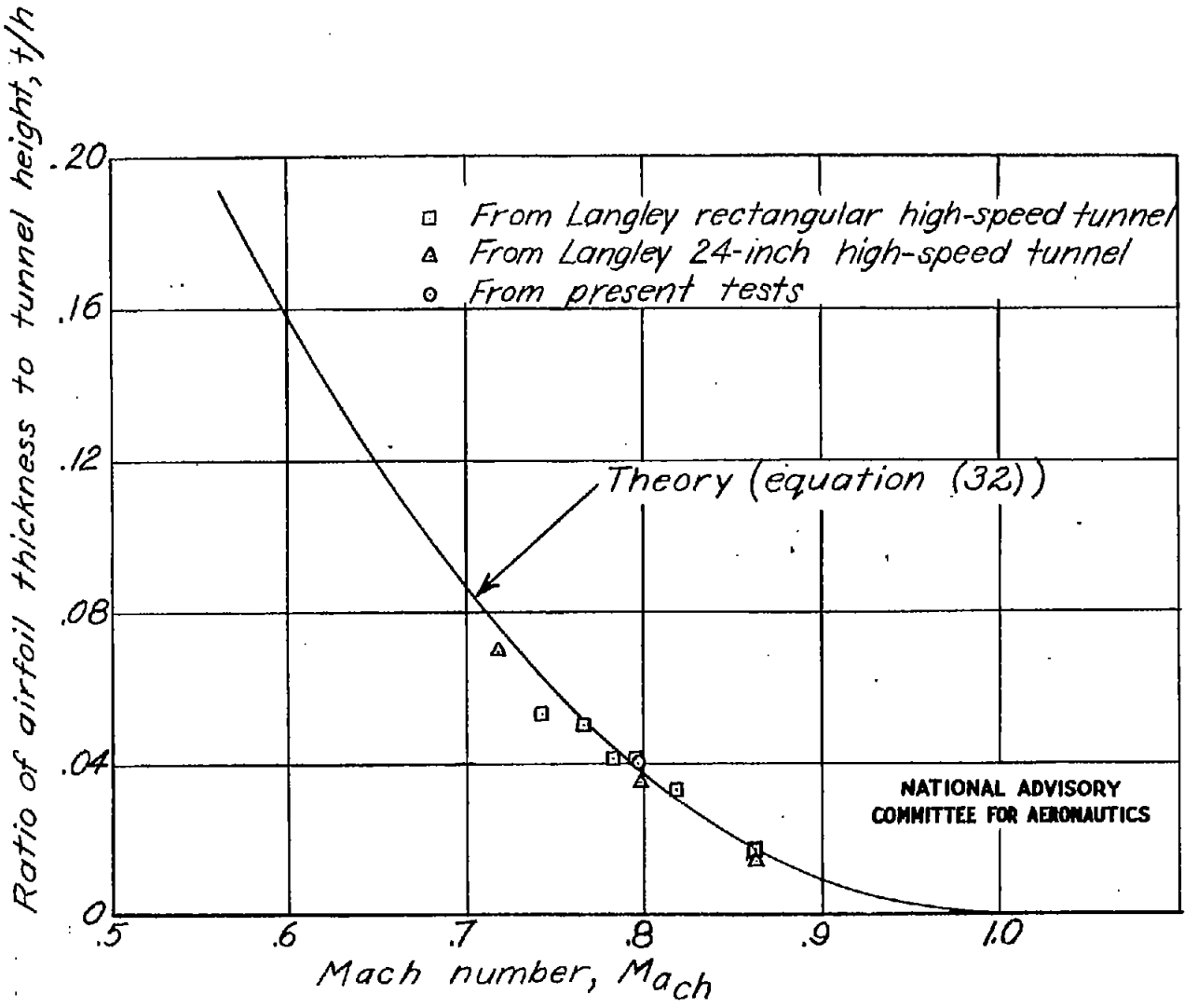

Figure 15.- Maximum Mach numbers attained in several Langley high-speed tunnels.

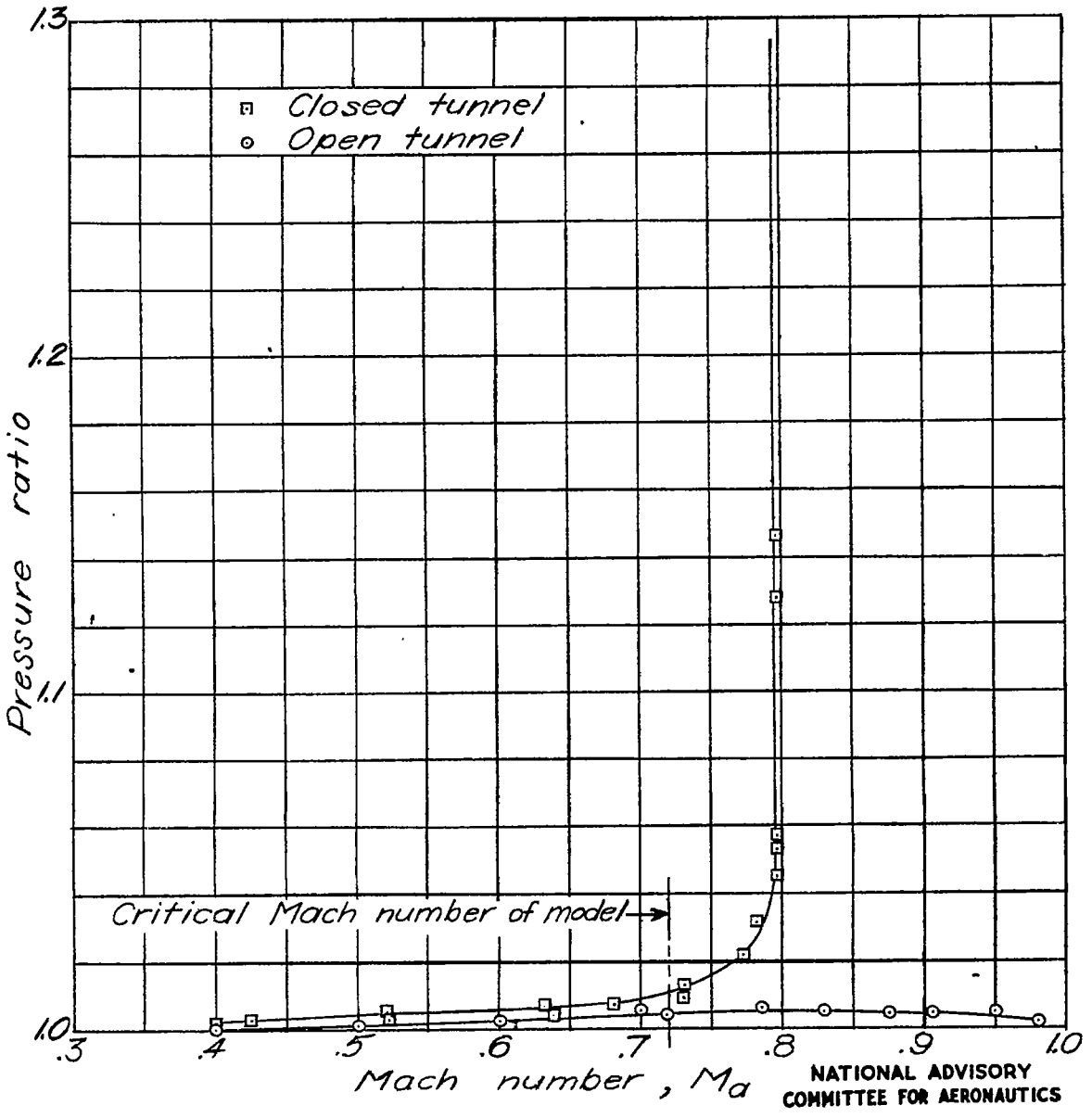

Figure 16.- Ratio of static pressure one chord ahead of model to static pressure one chord behind model.

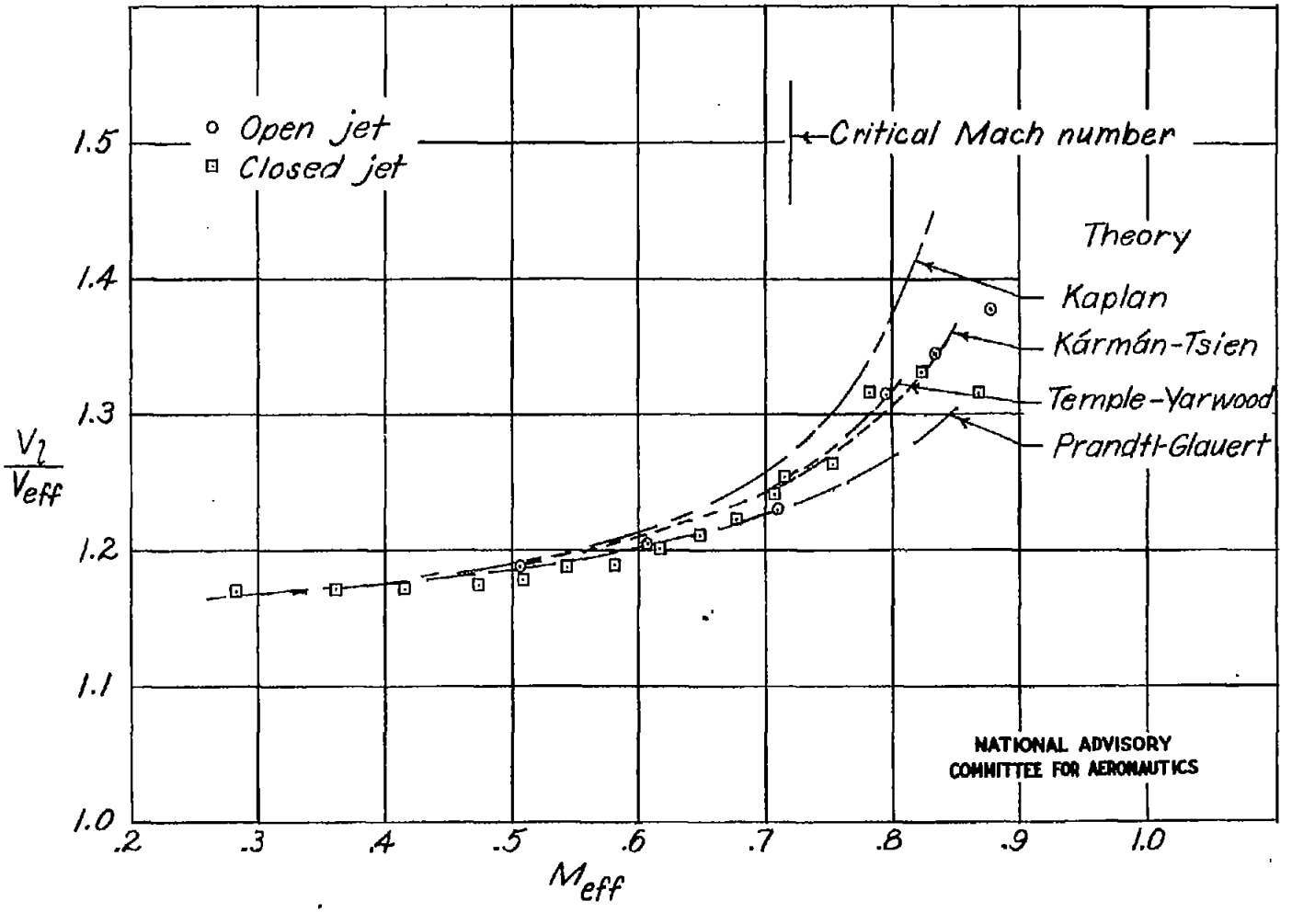

Figure 17.- Comparison of experimental and theoretical variation with Mach number M_{eff} of velocity ratio V_l/V_{eff} at 27.5-percent-chord station.

(Subscript eff designates effective values of velocity and Mach number corrected for wake and solid blockage and for influence of model at calibration orifices a and b.)